Ecotoxicology and Environmental Safety

ZnO nanoparticles induce cell wall remodeling and modify ROS/ RNS signalling in roots of Brassica seedlings

--Manuscript Draft--

Manuscript Number:	EES-20-2078R1
Article Type:	Research paper
Section/Category:	Ecotoxicology
Keywords:	Brassica juncea; Brassica napus; cell wall remodeling; nitro-oxidative signalling; zinc oxide nanoparticles
Corresponding Author:	Zsuzsanna Kolbert, Ph.D. Szegedi Tudomanyegyetem Termeszettudomanyi es Informatikai Kar Szeged, HUNGARY
First Author:	Árpád MOLNÁR
Order of Authors:	Árpád MOLNÁR
	Andrea RÓNAVÁRI
	Péter BÉLTEKY
	Réka SZŐLLŐSI
	Emil VALYON
	Dóra OLÁH
	Zsolt RÁZGA
	Attila ÖRDÖG
	Zoltán KÓNYA
	Zsuzsanna Kolbert, Ph.D.
Abstract:	Cell wall-associated defence against zinc oxide nanoparticles (ZnO NPs) as well as nitro-oxidative signalling and its consequences in plants are poorly examined. Therefore, this study compares the effect of chemically synthetized ZnO NPs (~45 nm, 25 or 100 mg/L) on Brassica napus and Brassica juncea seedlings. The effects on root biomass and viability suggest that B. napus is more tolerant to ZnO NP exposure relative to B. juncea . This may be due to the lack of Zn ion accumulation in the roots, which is related to the increase in the amount of lignin, suberin, pectin and in peroxidase activity in the roots of B. napus . TEM results indicate that root cell walls of 25 mg/L ZnO NP-treated B. napus may bind Zn ions. Additionally, callose accumulation possibly contribute to root shortening in both Brassica species as the effect of 100 mg/L ZnO NPs. Further results suggest that in the roots of the relatively sensitive B. juncea the levels of superoxide radical, hydrogen peroxide, hydrogen sulfide, nitric oxide, peroxinitrite and S-nitrosoglutathione increased as the effect of high ZnO NP concentration meaning that ZnO NP intensifies nitro-oxidative signalling. In B. napus; however, reactive oxygen species signalling was intensified, but reactive nitrogen species signalling wasn't activated by ZnO NPs.

Cover Letter

DEPARTMENT OF PLANT BIOLOGY
FACULTY OF SCIENCE
UNIVERSITY OF SZEGED
H-6726 SZEGED
HUNGARY
Phone/Fax: +36-62-544-307
E-mail: kolzsu@bio.u-szeged.hu
Dr. Zsuzsanna Ördögné Kolbert

Dear Editorial Board of *Ecotoxicology and Environmental Safety*,

Hereby, please find the revised version of our manuscript entitled „**ZnO nanoparticles induce cell wall modifications and modify ROS/ RNS signalling in roots of *Brassica* seedlings**" written by Árpád Molnár et al. for consideration to publish in EES.

We investigated ZnO nanoparticle induced cell wall modification in detail for the first time and provide new evidence for nitro-oxidative stress-inducing effect of ZnO nanoparticles in plants. Therefore, we believe that our study falls into the scope of the journal (ecotoxicology).

We revised the manuscript to our best knowledge and we are confident about its positive evaluation.

Szeged, 6th of August, 2020

Dr. Zsuzsanna Kolbert
Associate professor
Corresponding author

Responses to Reviewer's Comments

Reviewer #1: Comments to Authors:

The present paper investigates the effect of ZnO nanopartcles on cell wall remodeling and ROS/RNS signalling in roots of Brassica seedlings. Overall the paper is very interesting and complex with a lot of different laboratory methods that give a good insight in the topic. The novelty of the paper is the role of ZnO nanoparticles in modification of the cell wall (lignification, pectin accumulation, lignin-suberin deposition, callose accumulation) that is concentration and species-dependent. The paper is well written, the methods are described in detail and the results are clearly presented. The only minor objection is the Discussion part where some lack of explanations and possible mechanisms are present. The impact of higher dose of ZnO NP (100 mg/L) is well described and supported by previous research through the whole Discussion part. On the other hand, the impact of the lower ZnO NP dose is only mentioned in the text. The authors showed beneficial effect of low ZnO NP dose on root elongation in both species and fresh weight and root width in B. napus (Ln 268). In the same time (Ln320) the intra cellular Zn2+ level in the B. napus did not increase while POD activity increased and H2O2 level decreased. In the same time RNS system is not affected by this treatment (Fig 5C and Fig 6) . There are no possible explanations and mechanisms for this results nowhere in the Discussion part. When authors improve this part of the Discussion, in my opinion, the paper can be accepted for publishing in Ecotoxicology and Environmental Safety.

We highly appreciate the positive evaluation of our manuscript and we agree with the suggestion. We improved the discussion and conclusion parts by evaluating the results of the low NP dose in more detail.

Here we summarize our results obtained in case of 25 mg/L ZnO NP concentration as follows: In our opinion our results support that in the presence of 25 mg/L ZnO NP, *B. napus* alters its cell wall composition in order to be able to bind most of the Zn^{2+} in the apoplast. Due to the binding, intracellular Zn^{2+} levels only slightly elevates (creating beneficial concentrations) leaving the ROS and RNS homeostasis undisturbed. Thus the beneficial effect on growth and biomass production may prevail. In case of *B. juncea*, much slighter cell wall modifications are induced by the low ZnO NP dosage resulting in the notable elevation of intracellular Zn^{2+} level, in the accumulation of NO which may contribute to viability loss and to the mitigation of the beneficial effect of low ZnO NP concentration.

We changed the text as follows:

L 297-299: "*The above results indicate that 25 mg/L applied NP dose positively affected root biomass in both species; however, it was more significant in B. napus compared to B. juncea where root fresh weight and thickness remained at control-level and root viability decreased.*"

L 376-378: *"Collectively, the low ZnO NP concentration (25 mg/L) resulted in lignification, pectin and suberin accumulation in the roots of B. napus, which may contribute to the observed* Zn^{2+}*-binding in the cell wall and to the beneficial effect on root biomass production."*

L 419-424: *"The fact that the beneficial concentration of ZnO NPs didn't influence ROS and RNS levels in B. napus indicates that this species is able to maintain a healthy ROS/RNS homeostasis. In case of B. juncea, ROS levels are unaffected by the low ZnO NP dosage and GSNO decomposition may lead to the observed NO formation which doesn't induce protein nitration but may contribute to the mitigation of the beneficial effect of 25 mg/L ZnO NP in this species."*

L 444-449: *"Interestingly, both ZnO NP doses caused reduction in nitration level in the relative tolerant B. napus (indicated by decreased immunopositive signals) as well as in B. juncea exposed to low ZnO NP dose regardless of the state of ROS/RNS metabolism indicating that a process may regulate nitration level independently from ROS/RNS. Such mechanism can be the intensified proteasomal degradation of nitrated proteins reversing the damage (Tanou et al., 2012; Castillo et al., 2015)."*

L 463-466: *"Due to these alterations in cell wall composition,* Zn^{2+} *may be bounded by the cell walls. These may result in beneficially elevated* Zn^{2+} *levels in the cytoplasm of root cells which cause undisturbed ROS and RNS metabolism allowing the positive effects on biomass production."*

We highlighted all relevant changes in the manuscript by yellow color.

Graphical Abstract

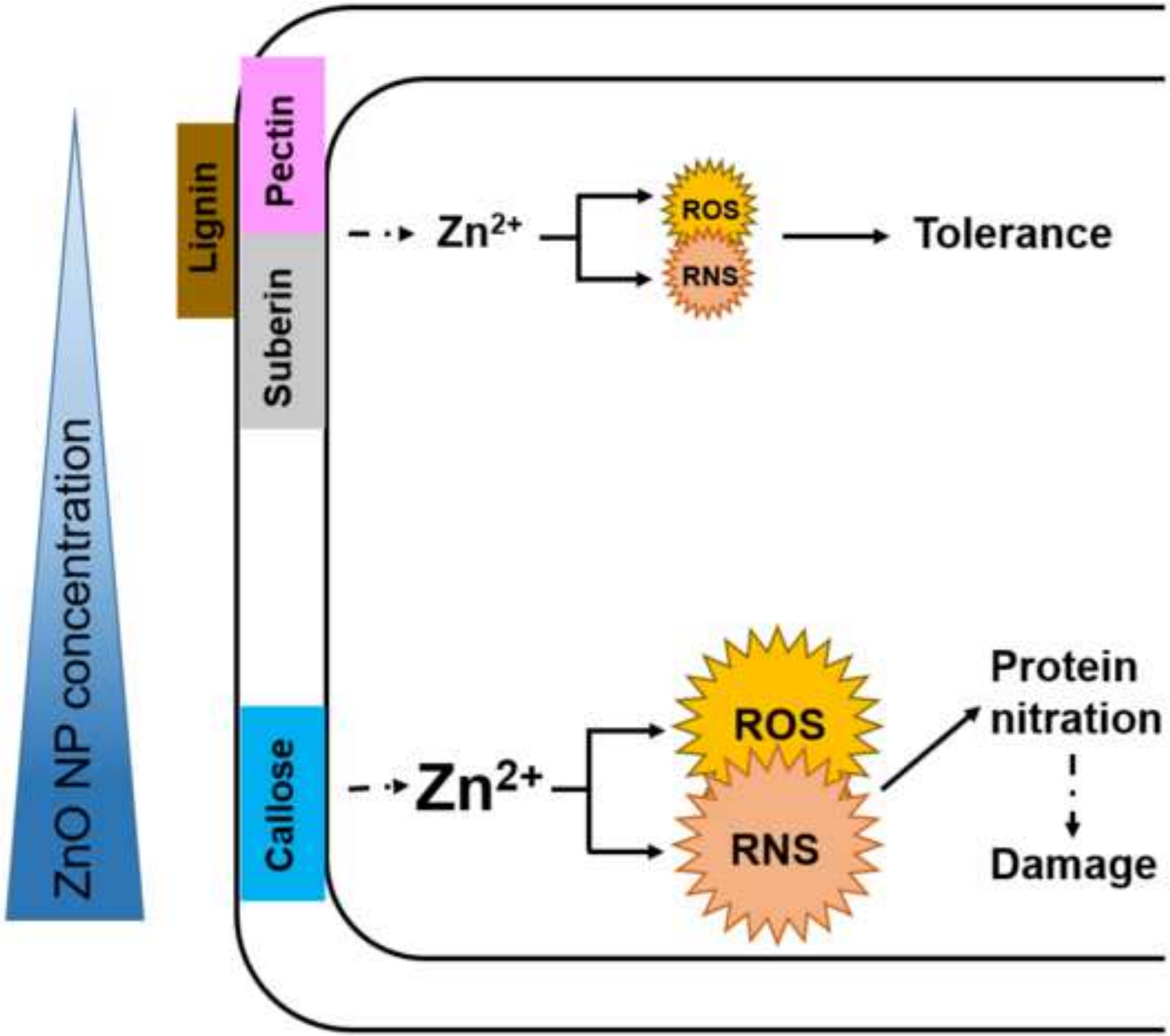

Highlights

- ZnO NPs induce cell wall modifications in the relatively tolerant *Brassica napus*
- Cell wall remodeling may contribute to Zn-binding and ZnO NP tolerance
- ZnO NPs disturb ROS/RNS metabolism in sensitive *B. juncea*
- Nitro-oxidative signalling is associated with ZnO NP tolerance of *Brassica* species

Title: ZnO nanoparticles induce cell wall remodeling and modify ROS/ RNS signalling in roots of *Brassica* seedlings

Árpád MOLNÁR[1], Andrea RÓNAVÁRI[2], Péter BÉLTEKY[2], Réka SZŐLLŐSI[1], Emil VALYON[1], Dóra OLÁH[1], Zsolt RÁZGA[3], Attila ÖRDÖG[1], Zoltán KÓNYA[2], Zsuzsanna KOLBERT[1]*

[1] Department of Plant Biology, Faculty of Science and Informatics, University of Szeged, H-6726 Szeged, Közép fasor 52., Hungary

[2] Department of Applied and Environmental Chemistry, Faculty of Science and Informatics, University of Szeged, H-6720 Szeged, Rerrich Bela ter 1., Hungary

[3] Department of Pathology, Faculty of Medicine, University of Szeged, H-6725 Szeged, Állomás u. 2., Hungary

*correspondence: Zsuzsanna Kolbert kolzsu@bio.u-szeged.hu

Árpád Molnár	molnara@bio.u-szeged.hu
Andrea Rónavári	ronavari@chem.u-szeged.hu
Péter Bélteky	beltekyp@chem.u-szeged.hu
Réka Szőllősi	szoszo@bio.u-szeged.hu
Emil Valyon	emil6555@citromail.hu
Dóra Oláh	olahdora.csorvas@gmail.com
Zsolt Rázga	razgazst44@hotmail.com
Attila Ördög	aordog@bio.u-szeged.hu
Zoltán Kónya	konya@chem.u-szeged.hu

Abstract

Cell wall-associated defence against zinc oxide nanoparticles (ZnO NPs) as well as nitro-oxidative signalling and its consequences in plants are poorly examined. Therefore, this study compares the effect of chemically synthetized ZnO NPs (~45 nm, 25 or 100 mg/L) on *Brassica napus* and *Brassica juncea* seedlings. The effects on root biomass and viability suggest that *B. napus* is more tolerant to ZnO NP exposure relative to *B. juncea*. This may be due to the lack of Zn ion accumulation in the roots, which is related to the increase in the amount of lignin, suberin, pectin and in peroxidase activity in the roots of *B. napus*. TEM results indicate that root cell walls of 25 mg/L ZnO NP-treated *B. napus* may bind Zn ions. Additionally, callose accumulation possibly contribute to root shortening in both *Brassica* species as the effect of 100 mg/L ZnO NPs. Further results suggest that in the roots of the relatively sensitive *B. juncea* the levels of superoxide radical, hydrogen peroxide, hydrogen sulfide, nitric oxide, peroxinitrite and S-nitrosoglutathione increased as the effect of high ZnO NP concentration meaning that ZnO NP intensifies nitro-oxidative signalling. In *B. napus;* however, reactive oxygen species signalling was intensified, but reactive nitrogen species signalling wasn't activated by ZnO NPs. Collectively, these results indicate that ZnO NPs induce cell wall remodeling which may be associated with ZnO NP tolerance. Furthermore, plant tolerance against ZnO NPs is associated rather with nitrosative signalling than oxidative modifications.

Keywords: *Brassica juncea*, *Brassica napus*, cell wall modifications, nitro-oxidative signalling, zinc oxide nanoparticles

1. Introduction

Zinc oxide nanoparticles (ZnO NPs) are released into the environment where sessile plants are particularly affected by their toxic effects. Plants can come in contact with ZnO NPs through foliage or mostly through their root system. In the presence of plant roots, ZnO NPs release Zn ions (Zn^{2+}) (López-Moreno et al., 2010) which are absorbed by the roots with specific transporters (Milner et al. 2013). The internalization of ZnO NPs smaller than cell wall pores (5-30 nm) may also happen (Fleischer et al., 1999; Nair et al., 2010) as well as the decomposition of larger NPs or aggregates into smaller ones. Additional mechanisms of NP uptake such as endocytosis, pore formation and carrier proteins-mediated internalization have been proposed (Pérez-de-Luque, 2017; Lv et al., 2019). Within the root tissue, ZnO NPs move *via* symplastic pathway involving plasmodesmata, although their root-to shoot translocation within the vascular tissues has not been supported by experimental data (Wang et al., 2013; Lv et al., 2015; Singh et al., 2018). ZnO NPs can positively or negatively affect root and shoot development depending on the concentration, particle size, surface area, stability, physicochemical properties, plant species and developmental stage (Singh et al., 2018; Sturikova et al., 2018).

Plants have the ability to actively protect their cells against stressors by modifying the composition and structure of their cell walls (Tenhaken, 2014; Le Gall et al., 2015; Houston et al., 2016). In general, cell wall remodeling form an effective barrier against heavy metal (HM) accumulation in the root tissues due to binding of HMs (pectin/lignin accumulation, Loix et al., 2017) or preventing symplastic (callose deposition, Vatén et al., 2011) or apolastic transport of HM ions (exodermal lignification and suberinization, Cheng et al., 2014). Cell wall-associated class III peroxidases (cwPOD) contribute to lignin and suberin formation due to oxidizing small phenolic compounds coniferyl, sinapyl, and p-coumaryl alcohols as precursors of lignin and ferulic acid, caffeic acid and p-coumaric acid as precursors of suberin (Shigeto and Tsusumi,

2016). Additionally, PODs oxidize flavonol substrates (Takahama and Oniki, 2000). Flavonols proved to be multitasking secondary metabolites protecting against UV-B radiation, regulating hormone levels and signalling, participating in metal binding depending on the chemical structure (Brown et al., 1998; Aherne and O'Brien, 2000; Soczynska-Kordala et al., 2001; Michalak, 2006; Korkina, 2007) and modulating reactive oxygen species (ROS) homeostasis together with PODs (Brunetti et al., 2019).

Overproduction of ROS (like hydrogen peroxide, H_2O_2 or superoxide radial, $O_2^{\cdot -}$) due to the downregulation of the antioxidant machinery leads to oxidative modification of proteins, nucleic acids and lipids. Lipid peroxidation can be considered as a marker of the intensification of ROS-mediated oxidative signalling (Foyer et al., 2017). Besides ROS, reactive nitrogen species (RNS) such as nitric oxide (NO), peroxynitrite ($ONOO^-$) and S-nitrosoglutathione (GSNO) as well as hydrogen sulfide (H_2S) as a representative of reactive sulphur species (RSS) are important modulators in the redox signalling matrix where ROS, RNS and RSS signalling is tightly connected (Hancock and Whiteman, 2016). Indeed, $ONOO^-$ is formed in the reaction between NO and $O_2^{\cdot -}$ (Vandelle and Delledonne, 2011) while the reaction of NO with glutathione yields GSNO (Khajuria et al., 2019). The bioactivity of RNS is transferred by posttranslational protein modifications such as *S*-nitrosation during which thiol groups in specific cysteines are reversibly converted into *S*-nitrosothiols by NO (Feng et al., 2019). During the irreversible protein nitration, mainly tyrosine amino acids are affected indirectly by $ONOO^-$ leading to the formation of 3-nitrotyrosine and as a result protein structure is modified and protein activity is lost in most known cases (Kolbert et al., 2017). The intensity of protein tyrosine nitration was found to be correlated with stress severity (Lehotai et al., 2016; Molnár et al., 2018a; b) and with the sensitivity of plant species (e.g. Kolbert el. al., 2018; 2020) thus protein nitration can be considered as a biomarker of nitrosative (or nitro-oxidative) signalling (Valderrama et al., 2007).

Despite the considerable amount of research data being accumulated in recent years on the effects of NPs on plants, the molecular mechanisms e.g. cell wall modifications or changes in nitro-oxidative signalling are poorly known. Thus, this study aims to investigate the effect of chemically synthesized ~45 nm ZnO NPs on cell wall composition, on cell wall-associated oxidative and on nitrosative signalling in a model system comparing *Brassica* species using *in situ* labelling techniques.

2. Materials and Methods

2.1.Chemical synthesis of ZnO NPs

ZnO nanoparticles were prepared based on the work of Srivastava et al. (2013). In a typical synthesis, 100 mL of 0.2 M zinc chloride was prepared in a beaker. Once the salt was completely dissolved, 25 % ammonia solution was dropwise added to the mixture under vigorous stirring until no further precipitation was observed (typically, the volume of the added ammonia solution was around 1.25 mL). This mixture was further stirred for 15 minutes, afterwards, the precipitate was washed once with ion exchanged water using ultracentrifugation. The precipitate was put in a drying oven on 60 °C overnight to remove any remaining solvent, then was ground with a hand mortar and calcinated at 450 °C for 2 h using a tube furnace in air. Ultimately, the product was once again ground into a fine powder and kept in room temperature until further use.

2.2.Characterization of ZnO NPs

To investigate the particle size, chemical composition and crystallinity of the synthesized nanoparticles, transmission electron microscopic (TEM) images and electron diffraction (ED) patterns were captured by a FEI Tecnai G^2 20 X-Twin instrument (FEI Corporate Headquarters, Hillsboro, OR, USA) using 200 kV accelerating voltage. The X-ray diffraction (XRD) of the prepared particles was measured to verify their composition by cross referencing their crystallinity with the literature using Cu Kα radiation in a Rigaku MiniFlex II powder diffractometer (Rigaku Corporation, Tokyo, Japan). Characteristic light absorbance properties were investigated with UV-Visible spectrophotometry by an Ocean Optics 355 DH-2000-BAL spectrophotometer (Halma PLC, Largo, FL, USA).

2.3.Preparation of ZnO NP treatment suspensions

In distilled water, adequate amount of ZnO NPs was dissolved, resulting in a heterogeneous suspension containing large ZnO NP aggregates, which was dispersed using an ultrasound sonicator. The pH of the treatment suspension was set to 5.7-5.8 and its volume was adjusted to a final concentration of 25 mg/L or 100 mg/L ZnO NP.

2.4.Plant material and growth conditions

Two *Brassica* species, Indian mustard (*Brassica juncea* L. Czern. cv. Negro Caballo) and oilseed rape (*Brassica napus* L. cv. GK Gabriella) were used as plant objects. Seeds were surface sterilized (70 v/v % ethanol of 1 min followed by 5% sodium hypochlorite for 15 min) and placed in Petri dishes (9 cm diameter) filled with filter paper. Filter paper was moistened with 5 ml distilled water (control) or with equal volume of aqueous solutions of ZnO NPs. Petri dishes were placed in control conditions (150 µmol m^{-2} s^{-1} photon flux density, 12h/12h light/dark cycle, relative humidity 55–60% and temperature 25±2 ºC) for 5 days. All analyses were performed using 5-day-old seedlings.

2.5.Determining root growth parameters and viability

Primary root length of *Brassica* seedlings was measured manually and expressed as centimetre (cm). Root fresh weight (FW) was measured using an analytical balance and expressed as milligram (mg). Root width (µm) was determined under microscope by measuring the diameter of root cross sections derived from the differentiation zone of the primary root. Viability of root meristem cells was estimated by labelling root tips with 10 µM fluorescein diacetate (FDA) solution for 30 min in the dark. Samples were washed four times in 20 min

with MES/KCl buffer (10 mM/50 mM, pH 6.15) and prepared on microscopic slides (Lehotai et al. 2011).

2.6. Visualization of cell wall components (callose, lignin, suberin, pectin), peroxidase activity and quercetin level in roots

For callose detection, root tips (~2 cm-long) were incubated in aniline blue solution (0.1% aniline blue (w/v) and 1 M glycine, dissolved in distilled water) for 5 min at room temperature in the dark (Cao et al., 2011) and washed once in distilled water. The level of lignin was visualized in the roots using phloroglucinol-HCl solution. Roots were incubated in 1 % (w/v) phloroglucinol solution prepared in 6 N HCl for 5 min, washed with distilled water and placed on slides (Rogers et al., 2005). Cross sections of roots were prepared similarly to Barroso et al. (2006). 5 mm pieces of mature roots were subjected to 4 % (w/v) paraformaldehyde fixative and then washed with distilled water. Samples were embedded in 5 % (w/v) bacterial agar according to the slightly modified method of Zelko et al. (2012). Embedded samples were cut with vibratome (VT 1000S, Leica) to acquire 100 µm thick root cross sections. Auramine-O staining was applied for the *in situ* visualization of lignin plus suberin in root cross sections prepared with vibratome. Cross sections were stained in dye solution (0.01% (w/v) prepared in 10 mM Tris-HCl buffer, pH 7.4) for 10 minutes in dark (Rahoui et al., 2017). Pectin content of root tips was visualised using Ruthenium Red (RR) according to Durand et al. (2009). Roots were incubated in 0.05 % (w/v) RR solution for 15 minutes, washed with distilled water and placed on slides. The activity of cell wall peroxidases (cwPODs) was detected with pyrogallol (Eleftheriou et al. 2015). Root tips were incubated for 15 min in staining solution (0.2 % w/v pyrogallol, 0.03 % (v/v) hydrogen peroxide, dissolved in 10 mM phosphate buffer, pH 7.0). Samples were washed two times and placed on slides with distilled water. Quercetin was visualized by incubating *Brassica* root tips in diphenylboric acid 2-amino-ethylester (DPBA)

solution (0.25 %(w/v) DPBA with 0.005 % (v/v) Triton X-100 prepared in distilled water) for 7 similarly to Sanz et al. (2014). Samples were washed with distilled water for 7 minutes once and placed on microscopic slides. Gold fluorescence corresponds to quercetin.

2.7.Estimation of free intracellular Zn^{2+} content in the roots and TEM analysis of ZnO NPs in *Brassica root* and *hypocotyl cells*

Zinc-specific fluorophore, Zinquin was used to detect free, intracellular Zn^{2+} in *Brassica* root tips. Specimens were stained with 25 µM Zinquin (prepared in 1 x PBS, pH 7.4) for 60 min at room temperature in the dark and washed once with buffer before placing on slides (Sarret et al., 2006). Segments from the mature zone of the root and from the hypocotyl were prepared and fixed with 3% glutardialdehyde (in PBS, pH 7.4). Following embedding in Embed812 (EMS, Hatfield, PA, USA), 70 nm thin sections were prepared with an Ultracut S ultra-microtome (Leica, Vienna, Austria). Specimens were stained with uranyl acetate and lead citrate, and the sections were observed with a Jeol 1400 plus transmission electron microscope (Jeol, Tokyo, Japan).

2.8.Determination ROS, hydrogen sulfide and RNS levels in *Brassica* roots

Dihidroethidium (DHE) was used for the detection of superoxide levels according to Kolbert et al. (2012). Samples were stained with 10 µM DHE solution (in 10 mM Tris-HCl buffer) and washed twice with buffer before microscopic analysis. Hydrogen peroxide levels were estimated with 50 µM 10-acetyl-3,7 dihydroxyphenoxazine (ADHP or Amplex Red) fluorescent probe solution prepared in 50 mM sodium phosphate buffer (pH 7.5). After staining the root tips were washed in buffer and placed on slides (Lehotai et al., 2012). Hydrogen sulfide was visualised using WSP-1 (Washington State Probe-1). Root tips were stained for 40 minutes in WSP-1 solution (15 µM, in 20 mM Hepes-NaOH buffer, pH 7.5), washed with distilled water

three times and examined under microscope (Li et al., 2014). The nitric oxide content of root tips was analysed with 4-amino-5-methylamino-2′,7′-difluorofluorescein diacetate (DAF-FM DA). Samples were stained for 30 minutes in fluorophore solution (10 µM, prepared in 10 mM Tris-HCl buffer, pH 7.4), washed two times with buffer and placed on slides (Kolbert et al., 2012). For the detection of peroxynitrite, aminophenyl fluorescein (APF) was used according to Chaki et al. (2009). 10 µM APF solution was prepared in 10 mM Tris-HCl and the root tips were incubated in it for 60 minutes. After incubation samples were washed two times with buffer and analysed under the microscope. The detection of S-nitrosogluthatone was performed on root cross sections prepared with vibratome as described above. Samples were incubated in 1:2500 rat anti-GSNO (VWR Chemicals, Poole, England) antibody prepared in TBSA-BSAT (5 mM Tris, 9% (w/v) NaCl, 0.05% (w/v) sodium azide, 0.1% (w/v) bovine serum albumin (BSA) and 0.1% (v/v) Triton X-100, pH 7.2) overnight at room temperature. After washing with buffer three times, 1:1000 anti-rat IgG antibody conjugated with fluorescein isothiocyanate (Agrisera, Vännäs, Sweden) was used as secondary antibody (Corpas et al., 2008). Cross sections were placed on slides with PBS:glycerine (1:1), and analysed under microscope. 250 µM GSNO treated sections were used as positive control and treated for 1 hour before immunohistochemistry.

2.9.Detection of 3-nitro-tyrosine and lipid peroxidation

Sections for 3-nitrotyrosine localisation were prepared as described above. As primary antibody, anti-3-nitrotyrosine (polyclonal, produced in rabbit, Sigma-Aldrich, St. Louis, USA) was used. Samples were incubated in 1:300 antibody solution (prepared in TBSA-BSAT) for 3 days at 4 ^{o}C. Cross sections were washed three times and labelled with 1:1000 FITC conjugated goat anti-rabbit IgG antibody (Agrisera, Vännäs, Sweden). Samples were examined on microscopic slides in PBS:glycerin 1:1 solution. As positive and negative controls of antibody

specificity, 1 mM 3-morpholino-sydnonimine (SIN) and 2 mM urate treatment was applied before the primary antibody staining (Kolbert et al., 2018).

Commercial Schiff reagent was used to detect lipid peroxidation in root tips. Samples were incubated in staining solution for 20 minutes, which was changed to $K_2S_2O_5$ solution (0.5 % (w/v) in 0.05 M HCl) for 20 minutes. After the staining, root tips were examined under microscope (Arasimowicz-Jelonek et al., 2009).

2.10. Microscopy

All analyses were performed using Axiovert 200M invert fluorescent microscope (Carl Zeiss, Jena, Germany). Filter set 10 (exc.: 450–490, em.: 515–565 nm) was used for FDA, DAF-FM, APF, Auramine-O and for FITC, filter set 9 (exc.:450–490 nm, em.:515–∞ nm) for DHE, DPBA, filter set 20HE (exc.: 546/12 nm, em.: 607/80 nm) for ADHP and filter set 36 (exc. em.) for Zinquin and aniline blue. Pixel intensity was measured in area of circles. The radii of circles were set in order to cover the largest sample area. Axiovision Rel. 4.8 software (Carl Zeiss, Jena, Germany) was applied for measuring of the pixel intensity on digital photographs.

2.11. Statistical analysis

All results are shown as mean values of raw data (±SE). For statistical analysis, Duncan's multiple range test (OneWay ANOVA, $P<0.05$) was used in SigmaPlot 12. For the assumptions of ANOVA, we used Hartley's F_{max} test for homogeneity and Shapiro-Wilk normality test.

3. Results and Discussion

3.1.NP synthesis and characterization

The TEM image of ZnO NPs (Supplementary Fig 1A) demonstrated that quasi-spherical nanoparticles could be formed using this simple synthesis method, with an average diameter of ~45 nm illustrated by their size distribution histogram (Supplementary Fig 1C). The ED and XRD results (Supplementary Fig 1B) that were collected to verify the crystallinity and chemical composition of the particles were analogous with one another and proved to be in good agreement with the literature (Talam et al., 2012; Kumar et al., 2013; Zhang et al., 2014; Ersan et al., 2015), thus confirming the synthesis product as nanosized zinc oxide. The observed UV-Vis spectra further proved the chemical composition of the sample, as an absorption maximum around 370 nm is a characteristic value according to the literature (Talam et al., 2012; Kumar et al., 2013).

It is worth mentioning, that all our results showed strong resemblance to one of our recent contributions (Molnár et al., 2020), where smaller (~8 nm) ZnO NPs were synthesized. While zinc oxide nanoparticles from both projects demonstrated similar XRD and UV-Vis characteristics, some discrepancies were observed that can highlight how particle size may affect certain properties. The full width at half maximum (FWHM) of XRD reflexion peaks decrease with increasing particle size, due to the higher amount of similar crystal facets, and the exact wavelength of the light absorption maximum of the characteristic UV-Vis spectra is also NP size dependent. Due to their larger size, the ZnO NPs discussed in this research possess sharper, more defined XRD reflexions and a moderately red shifted UV-Vis maximum compared to smaller (and perhaps more commonly investigated) particles. Based on these observations, the assumption could be made, that the as-prepared particles of this research may have other distinct characteristics, which could affect biological activity.

3.2.The effects of ZnO NPs doses on biomass production is similar in *Brassica species*

During stress-free circumstances, the primary root length of *B. juncea* is significantly smaller than that of *B. napus* (Fig 1A and D). The beneficial effect of low ZnO NP dose (25 mg/L) proved to be similar in both *Brassica* species, since it induced primary root (PR) elongation by 35-40%. High ZnO NP concentration (100 mg/L) caused PR shortening by 85% in *B. juncea*, while in *B. napus*, the negative effect proved to be significantly slighter (53%). The tendencies in ZnO NP-triggered changes of root fresh weight were similar to changes in PR length. The ZnO NPs at 25 mg/L concentration induced 20-25% increase in root fresh weight of both species; however, this was significant only in *B. napus* (Fig 1B). As the effect of 100 mg/L ZnO NP root fresh weight decreased by 74% in *B. juncea*, and by 46% in *B. napus*. Interestingly, ZnO NP treatments exerted no significant effects on shoot fresh weight compared to controls (data not shown). Root shortening was accompanied by root thickening in both species as indicated by the cross sections prepared from the differentiation zone of the primary root (Fig 1E). In case of *B. napus*, root width significantly increased as the effect of both ZnO NP concentrations (Fig 1C). *Brassica juncea* seedlings grown in the presence of 25 mg/L ZnO NP did not show significantly thickened roots, however, 100 mg/L ZnO NP exposure notably increased root width.

Viability of root meristem tissues significantly decreased (by 50-60%) due to 100 mg/L ZnO NP exposure in both species, but the low ZnO NP dose caused 35% reduction in *B. juncea* and practically no decrease in *B. napus* compared to control (Fig 2).

The above results indicate that 25 mg/L applied NP dose positively affected root biomass in both species; however, it was more significant in *B. napus* compared to *B. juncea* where root fresh weight and thickness remained at control-level and root viability decreased. The four-times higher ZnO NP concentration has detrimental effects on root biomass which are more pronounced in *B. juncea* compared to *B. napus*. Beneficial and toxic concentrations of

ZnO NPs slightly differ among experimental conditions, but in general, low doses (1-50 mg/L) ZnO NPs induce germination, seedling growth, shoot and root biomass of *Brassica* species while higher doses (>50 mg/L) reduce those parameters (Lin and Xing, 2007; Kouhi et al., 2014; Zafar et al., 2016; Rahmani et al., 2016; Singh et al., 2017) similarly to our results. Thickening of the primary root indicates that secondary cell wall modifications may have occurred (Somssich et al., 2016) in the presence of ZnO NPs which may influence Zn^{2+} uptake.

3.3.ZnO NPs-induced Zn^{2+} uptake and cell wall modifications in roots of *Brassica* seedlings

Due to biotransformation in the presence of the root, ZnO NPs release Zn^{2+} which is taken up by the root (Ma et al., 2013; Kouhi et al., 2015). Free, intracellular Zn^{2+} levels were visualized using Zinquin fluorophore (Fig 3A and B). Despite the increasing external ZnO NP concentrations, the intracellular Zn^{2+} level in *B. napus* roots did not increase, but in *B. juncea*, both 25 and 100 mg/L ZnO NP caused two-fold elevation of Zn^{2+} levels compared to control. Elevation in tissue Zn^{2+} level due to Zn^{2+} release from ZnO NPs was observed, *inter alia*, in maize (Lv et al., 2015; Wang et al., 2016), alfalfa (Bandyopaghyay et al., 2015) and wheat (Dimkpa et al., 2012).

Next, we examined whether the presence of ZnO NPs in root and stem cells (especially in cells walls) can be detected. Nanoparticles with the size of ~45 nm possibly cannot enter the cell wall pores having 5-30 nm width; however, their degradation to smaller NPs due to biotransformation is conceivable (Fleischer et al., 1999; Nair et al., 2010). The TEM images revealed that cell walls in case of 25 mg/L ZnO NP-treated *B. napus* became electron dense indicating the possible binding of NPs (indicated by white arrows in Fig 3C). This was not observed in root samples of 25 mg/L ZnO NP-exposed *B. juncea*. In root cells of untreated plants and in hypocotyl cells, no signs of NP internalization were found in TEM images (Fig

3C and D) supporting the immobility of ZnO NPs between root and shoot (Wang et al., 2013; Lv et al., 2015; Singh et al., 2018). Presumably, cell wall remodeling may contribute to Zn ion binding and to the prevention of ZnO NP internalization.

Plant cell wall is a flexible macromolecule complex and its composition is finely regulated but can be adapted to the environmental cues (Zhao et al., 2019). Cell wall modifications permit the bounding and exclusion of heavy metals from the sensitive cytoplasm.

In both species treated with 100 mg/L ZnO NP, callose accumulation was detected in walls of root tip cells as indicated by the elevation of callose-associated fluorescence (Fig 4A and B). Additionally, 25 mg/L ZnO NP treatment caused no effect in callose level of both species. Callose regulates the permeability of plasmodesmata and consequently the intercellular transport (Vatén et al., 2011). In the study of Yanik and Vardar (2015) callose accumulation was correlated with growth inhibition in the root of Al_2O_3 nanoparticles. Therefore, we suspect that in *Brassica* species, 100 mg/L ZnO NP-induced callose accumulation may contribute to the serious root shortening due to the reduction of symplastic molecule movement *via* plasmodesmata. There was no correlation between Zn^{2+} levels and callose accumulation in ZnO NP-treated *Brassica* suggesting that callose accumulation is potentially not involved in Zn^{2+} binding; however, callose may inhibit their movement *via* plasmodesmata. Lignification might form an effective barrier against heavy metals preventing their entry into the cytoplasm, and lignin also binds heavy metals (Parrotta et al., 2015; Loix et al. 2017). Lignin accumulation in cells walls was microscopically detectable in root differentiation zone of *B. napus* exposed to 25 mg/L or 100 mg/L ZnO NP (Fig 4C). In contrast, *B. juncea* roots showed no detectable ZnO NP-induced lignification. Lignin enrichment in the cell walls of the elongation zone may be partly responsible for root growth diminution in the presence of heavy metals (Schützendübel et al., 2001). In *B. napus,* lignin deposition was detected in the root parts close to the shoot, thus ZnO NP-induced lignification may not have a role in root growth inhibition in this experimental

system. Among nanomaterials, CuO NPs has been found to trigger lignin and callose accumulation in *S. lycopersicum*, *B. oleracea* (Singh et al., 2017) and *A. thaliana* (Nair and Chung, 2014).

Pectin is a component of the cell wall matrix with a complex structure having high water and Ca^{2+} binding properties (Voragen et al., 2009). Similar to lignification, pectin content was significantly increased by 25 mg/L ZnO NP treatment in *B. napus* roots (Fig 4D). Moreover, slight induction of pectin formation was detectable by Ruthenium Red staining also in *B. juncea* in case of both ZnO NP doses. Accumulation of pectic substances in the cell walls may result in more efficient Zn^{2+} binding due to the replacement of bounded Ca^{2+} (Dronett et al., 1996; Krezlowska, 2011; Loix et al., 2017). Based on this, we can assume that ZnO NP-induced formation of pectin in *B. napus* roots may result in Zn^{2+} binding in the cell wall and consequently its exclusion from the cytoplasm. Auramine-O staining can be applied for *in situ* visualization of suberin and lignin in cell walls. In cross sections from the differentiation root zones of both species, lignin and suberin-associated fluorescence increased as the effect of 100 mg/L ZnO NP exposure; however, the induction was more pronounced in *B. napus* (Fig 4E and F). As for the lower ZnO NP dose, it induced lignin and suberin deposition in the root cell walls of *B. napus*, but it decreased it in *B. juncea* (Fig 4E and F). Generally, lignin/suberin deposition within the exodermis significantly contributes to the formation of an apoplastic transport barrier (Hose et al., 2001). In roots of 25 and 100 mg/L ZnO NP-exposed *B. napus* the appearance of exodermal lignin/suberin was detectable suggesting the role of this cell wall modification in delaying Zn^{2+} entry into the roots as suggested by Cheng et al. (2014). Our results strengthen the hypothesis that lignification/suberinization correlates with metal tolerance (Cheng et al., 2014) since the more tolerant *B. napus* showed more pronounced lignin/suberin deposition compared to the relative sensitive *B. juncea*.

Collectively, the low ZnO NP concentration (25 mg/L) resulted in lignification, pectin and suberin accumulation in the roots of *B. napus*, which may contribute to the observed Zn^{2+}-binding in the cell wall and to the beneficial effect on root biomass production. Callose deposition was triggered only by the high ZnO NP dose in both *Brassica* species. Based on these, *B. napus* shows more intense cell wall modification due to ZnO NP treatment.

Additional cell-wall related defence processes such as flavonol contents and peroxidase activities were examined. Flavonols play multifunctional roles during heavy metal stress since they act as antioxidants in co-operation with cell wall peroxidases (cwPOD) and as chelators they bind metals (Brown et al., 1998; Aherne and O'Brien, 2000; Soczynska-Kordala et al., 2001; Michalak, 2006; Korkina, 2007; Cherrak et al., 2016). Additionally, flavonols regulate auxin transport consequently influencing growth (Gayomba et al., 2017). Elevation in quercetin levels was detectable only in *B. juncea* roots exposed to 100 mg/L ZnO NP (Fig 5A and B), while *B. napus* roots did not accumulate this flavonol molecule even in the presence of ZnO NPs. Beyond their participation in lignification and suberinization, cell wall-associated class III peroxidases (cwPODs) can oxidize flavonol substrates and convert H_2O_2 into H_2O (Liox et al., 2017). In 100 mg/L ZnO NP-treated *B. juncea*, quercetin accumulation was accompanied by decreased activity of cwPOD compared to control (Fig 5C) suggesting that cwPOD activity and quercetin levels are associated and inactivation of cwPOD may contribute to quercetin induction under ZnO NP stress (Fig 5A and B). Since cwPODs exert additional antioxidant functions, it is not surprising that the 25 mg/L ZnO NP-induced slight cwPOD activation (Fig 5C) was accompanied by unmodified quercetin levels (Fig 5A and B). Similar to ZnO NP, Ag NP treatment also caused activation of cwPODs in the leaves of *Halophila stipulacea* as indicated by the intensification of pyrogallol staining (Mylona et al., 2020).

3.4.ZnO NPs induce species specific alterations in ROS and RNS signalling

Cell wall PODs oxidize H_2O_2 and this reaction may contribute to the notable depletion of H_2O_2 levels in the root tips of both *Brassica* species treated with 25 mg/L ZnO NP (Fig 6A and G). The level of superoxide increased in both species as the effect of high ZnO NP dose, while 25 mg/L ZnO NP resulted in control-like superoxide levels (Fig 6B and G). The changes in the level of H_2S were similar in the species, since only 100 mg/L ZnO caused significant induction; although, this was more intense in *B. juncea* (Fig 6C). Endogenous production of H_2S has been reported in plants exposed to heavy metals and in some cases increased H_2S level correlated with heavy metal tolerance (Li et al., 2016). However, the fact that H_2S production was detected in 100 mg/L ZnO NP-exposed *B. juncea* roots suffering the most intense damages indicates that H_2S may contribute to stress rather than to tolerance. Interestingly, the ZnO NP concentrations did not influence NO levels in *B. napus* (Fig 6D and G), while the originally higher NO content in *B. juncea* roots further increased due to ZnO NP concentrations. The level of $ONOO^-$ in ZnO NP-exposed *B. napus* was control-like and it increased in *B. juncea* roots only as the effect of 100 mg/L ZnO NP treatment (Fig 6E). Similarly, GSNO level was unaffected by ZnO NP in *B. napus* (Fig 6F and G). Contrary, in *B. juncea* exposed to 25 mg/L ZnO NP decreased GSNO level was detected (Fig 6F and G) which may contribute to the increased NO level (Fig 6D and G). Additionally, high ZnO NP dose resulted in significantly increased GSNO content in *B. juncea* roots compared to control.

The fact that the beneficial concentration of ZnO NPs didn't influence ROS and RNS levels in *B. napus* indicates that this species is able to maintain a healthy ROS/RNS homeostasis. In case of *B. juncea*, ROS levels are unaffected by the low ZnO NP dosage and GSNO decomposition may lead to the observed NO formation which doesn't induce protein nitration but may contribute to the mitigation of the beneficial effect of 25 mg/L ZnO NP in this species.

It was an interesting tendency that as the effect of the high ZnO NP dose, the level of the examined ROS ($O_2^{\cdot-}$ and H_2O_2) and also the level of H_2S altered similarly in both *Brassica* species; although ZnO NP-induced changes in the level of the examined RNS (NO, $ONOO^-$, GSNO) showed species dependency. In *B. napus* roots, the RNS homeostasis is unchanged, but in *B. juncea* the RNS metabolism is disturbed and RNS overproduction occurred in the presence of high ZnO NP dosage. Nanoparticle-induced disturbance of ROS homeostasis due to altered antioxidant functions have been documented in several plant species (Thwala et al., 2013; Vannini et al., 2013; Fu et al., 2014; Mirzajani et al., 2014; Hossain et al., 2015; Xia et al., 2015; Ghosh et al. 2016; Jiang et al., 2017; Tripathi et al., 2017, Marslin et al., 2017), although nitrosative processes in NP-treated plants are much less known. In duckweed, NP-triggered NO production was detected (Thwala et al., 2013) similarly to ZnO NP-treated *B. juncea*. Our previous work revealed that ~8 nm ZnO NPs triggered the same alteration in NO and also in $ONOO^-$ levels in *Brassica* species as by the ~44 nm NPs suggesting that NO and $ONOO^-$ production is independent from the particle size of ZnO NP. Zinc-induced iron deficiency can be responsible for NO production as was observed in the roots of *Solanum nigrum* (Xu et al., 2010).

As a result of RNS imbalance, tyrosine nitration was observed in roots of 100 mg/L ZnO NP-treated *B. juncea* (Fig 7A and B), where simultaneous ROS and RNS overproduction was detected supporting the hypothesis that tyrosine nitration can be considered as a biomarker for nitro-oxidative signalling (Valderrama et al., 2007). Interestingly, both ZnO NP doses caused reduction in nitration level in the relative tolerant *B. napus* (indicated by decreased immunopositive signals) as well as in *B. juncea* exposed to low ZnO NP dose regardless of the state of ROS/RNS metabolism indicating that a process may regulate nitration level independently from ROS/RNS. Such mechanism can be the intensified proteasomal degradation of nitrated proteins reversing the damage (Tanou et al., 2012; Castillo et al., 2015).

Similarly, to tyrosine nitration, lipid peroxidation was mostly detectable in roots of *B. juncea* treated with 100 mg/L ZnO NP (Fig 7C). However, in case of both *Brassica* species there were Schiff reagent-labelled roots. In case of 100 mg/L ZnO NP-treated *B. napus,* approx. 33% of the root tips showed Schiff staining, while in case of *B. juncea* approx. 66% of the root tips were positively stained by the Schiff reagent indicating that ZnO caused more intense lipid peroxidation in *B. juncea* than in *B. napus*. Our results support previous findings regarding the lipid peroxidation-inducing effect of NPs in *Triticum aestivum*, *Oryza sativa*, *Nitzschia closterium*, *Vicia faba*, *Nicotiana tabacum*, *Glycine max* and *Solanum lycopersicum* (Dimkpa et al., 2012; Shaw and Hossein, 2013; Xia et al., 2015; Hashemi et al., 2019).

4. Conclusion

Collectively, this study revealed concentration and species-dependent effects of chemically synthetized ZnO NPs in *Brassica* seedlings. Results showed for the first time that the beneficial ZnO NP dose (25 mg/L) triggers cell wall modifications (lignification, pectin accumulation, lignin-suberin deposition, cwPOD activity) in relatively tolerant *B. napus*. Due to these alterations in cell wall composition, Zn^{2+} may be bounded by the cell walls. These may result in beneficially elevated Zn^{2+} levels in the cytoplasm of root cells which cause undisturbed ROS and RNS metabolism allowing the positive effects on biomass production. The root shortening induced by the high ZnO NP dose (100 mg/L) in both species may be associated with callose accumulation-induced inhibition of symplastic transport. Moreover, POD activation as the effect of high ZnO NP dose may contribute to quercetin level increase in the roots of *B. juncea*. Further results indicate that *B. juncea* roots suffer more severe ZnO-induced damage, as the levels of $O_2^{\cdot-}$, H_2O_2, H_2S, NO, $ONOO^-$ and GSNO increased with high ZnO NP concentration, suggesting that ZnO NP intensifies nitro-oxidative signalling. In contrast, *B. napus* showed better performance in the presence of ZnO NPs; ROS signalling intensified, but

RNS signalling was not activated by ZnO NPs. These results indicate that plant tolerance against ZnO NPs is associated with nitrosative signalling.

Funding:

This work was financed by the National Research, Development and Innovation Fund [Grant no. NKFI-8, KH129511]. Zs. K. was supported by the János Bolyai Research Scholarship of the Hungarian Academy of Sciences [Grant no. BO/00751/16/8]. A. Molnar was supported by UNKP-19-3-SZTE-201 New National Excellence Program of the Ministry for Innovation and Technology.

Acknowledgements:

The authors thank Éva Kapásné Török for her valuable assistance during the experiments.

References

Aherne, S.A., O'Brien, N.M., 2000. Mechanism of protection by the flavonoids, quercetin and rutin, against tert-butylhydroperoxide- and menadione-induced DNA single strand breaks in Caco-2 cells. Free Radic. Biol. Med. 29, 507-514.

Arasimowicz-Jelonek, M., Floryszak-Wieczorek, J., Kubiś, J., 2009. Involvement of nitric oxide in water stress-induced responses of cucumber roots. Plant. Sci. 177, 682–690.

Barroso, J.B., Corpas, F.J., Carreras, A., Rodríguez-Serrano, M., Esteban, F.J., Fernandez-Ocana, A., 2006. Localization of S-nitrosoglutathione and expression of S-nitrosoglutathione reductase in pea plants under cadmium stress. J. Exp. Bot. 57, 1785–1793.

Brown, J.E., Khodr, H., Hider, R.C., Rice-Evans, C.A., 1998. Structural dependence of flavonoid interactions with Cu(II) ions: implication for their antioxidant properties. Biochem. J. 359, 1173–1178.

Brunetti, C., Sebastiani, F., Tattini, M., 2019. Review: ABA, flavonols, and the evolvability of land plants. Plant Sci. 280, 448-454.

Cao, Y., Lou, Y., Han, Y., Shi, J., Wang, Y., Wang, W., Ming, F., 2011. Al toxicity leads to enhanced cell division and changed photosynthesis in *Oryza rufipogon* L. Mol. Biol. Rep. 38, 4839. http://doi.org/10.1007/s11033-010-0618-9

Castillo, M.C., Lozano-Juste, J., González-Guzmán, M., Rodriguez, L., Rodriguez, P.L., León, J., 2015. Inactivation of PYR/PYL/RCAR ABA receptors by tyrosine nitration may enable rapid inhibition of ABA signaling by nitric oxide in plants. Sci. Signal. 8(392), ra89. https://doi.org/10.1126/scisignal.aaa7981

Chaki, M., Valderrama, R., Fernández-Ocaña, A.M., Carreras, A., López-Jaramillo, J., Luque, F., Palma, J.M., Pedrajas, J.R., Begara-Morales, J.C., Sánchez-Calvo, B., Gómez-Rodríguez, M.V., Corpas, F.J., Barroso, J.B., 2009. Protein targets of tyrosine nitration in sunflower *(Helianthus annuus L.)* hypocotyls. J. Exp. Bot. 60, 4221–4234.

Cheng, H., Jiang, Z.-Y., Liu, Y., Ye, Z.-H., Wu, M.-L., Sun, C.-C., Sun, F.-L., Fei, J., Wang, Y.-S., 2014. Metal (Pb, Zn and Cu) uptake and tolerance by mangroves in relation to root anatomy and lignification/suberization. Tree Physiol. 34, 646–656.

Cherrak, S.A., Mokhtari-Soulimane, N., Berroukeche, F., Bensenane, B., Cherbonnel, A., Merzouk, H., Elhabiri, M., 2016. *In vitro* antioxidant versus metal ion chelating properties of flavonoids: a structure-activity investigation. PLoS ONE 11, e0165575. https://doi.org/10.1371/journal.pone.0165575

Corpas, F.J., Carreras, A., Esteban, F.J., Chaki, M., Valderrama, R., del Río, L.A., Bassoso, J.B., 2008. Localization of S-nitrosothiols and assay of nitric oxide synthase and S-nitrosoglutathione reductase activity in plants. Methods Enzymol. 437, 561–574.

Dimkpa, C.O., McLean, J.E., Latta, D.E., Manangón, E., Britt, D.W., Johnson, W.P., Boyanov, M.I., Anderson, A.J., 2012. CuO and ZnO nanoparticles: phytotoxicity, metal speciation, and induction of oxidative stress in sand-grown wheat. J. Nano. Res. 14, 1125. https://doi.org/10.1007/s11051-012-1125-9

Dronnet, V.M., Renard, C.M.G.C., Axelos, M.A.V., Thibault, J.F., 1996. Heavy metals binding by pectins: selectivity, quantification and characterization. Carbohydr. Polym. 30, 253–263.

Durand, C., Vicré-Gibouin, M., Follet-Gueye, M.L., Duponchel, L., Moreau, M., Lerouge, P., Driouich, A., 2009. The organization pattern of root border-like cells of *Arabidopsis* is dependent on cell wall homogalacturonan. Plant Physiol. 150, 1411–1421.

Eleftheriou, E.P., Adamakis, I.-D., Panteris, E., Fatsio, M., 2015. Chromium-induced ultrastructural changes and oxidative stress in roots of *Arabidopsis thaliana*. Int. J. Mol. Sci. 16, 15852–15871.

Ersan, A.C., Yildirim, M., Kipcak, A.S., Tugrul, N., 2019. A novel synthesis of zinc borates from a zinc oxide precursor via ultrasonic irradiation. Acta Chim. Slov. 63, 881-890.

Feng, J., Chen, L., Zuo, J., 2019. Protein S-Nitrosylation in plants: Current progresses and challenges. J Integr. Plant Biol. 61, 1206-1223.

Fleischer, A., O'Neill, M.A., Ehwald, R., 1999. The Pore size of non-graminaceous plant cell walls is rapidly decreased by borate ester cross-linking of the pectic polysaccharide rhamnogalacturonan II. Plant Physiol. 121, 829-838.

Foyer, C., Ruban, A.V., Noctor, G., 2017. Viewing oxidative stress through the lens of oxidative signalling rather than damage. Biochem J. 474, 877-883.

Fu, P.P., Xia, Q., Hwang, H.M., Ray, P.C., Yu, H., 2014. Mechanisms of nanotoxicity: generation of reactive oxygen species. J. Food. Drug Anal. 22, 64–75.

Gayomba, S.R., Watkins, J.M., Muday, G.K., 2017. Flavonols regulate plant growth and development through regulation of auxin transport and cellular redox status. In: Recent Advances in Polyphenol Research, edited by Kumi Yoshida, Véronique Cheynier, Stéphane Quideau, John Wiley and sons Ltd. pp 143-170.

Ghosh, M., Jana, A., Sinha, S., Jothiramajayam, M., Nag, A., Chakraborty, A., Mukherjee, A., Mukherjee, A., 2016. Effects of ZnO nanoparticles in plants: Cytotoxicity, genotoxicity, deregulation of antioxidant defenses, and cell-cycle arrest. Mutat. Res. Genet. Toxicol. Environ. Mutagen. 807, 25-32.

Hancock, J.T., Whiteman, M., 2016. Hydrogen sulfide signaling: Interactions with nitric oxide and reactive oxygen species. Ann. N Y Acad. Sci. 1365, 5-14.

Hashemi, S., Asrar, Z., Pourseyedi, S., Nadernejad, N., 2019. Investigation of ZnO nanoparticles on proline, anthocyanin contents and photosynthetic pigments and lipid peroxidation in the soybean. IET Nanobiotechnol. 13, 66-70.

Hose, E., Clarkson, D.T., Steudle, E., Schreiber, L., Hartung, W., 2001. The exodermis: a variable apoplastic barrier. J. Exp. Bot. 52, 2245–2264.

Hossain, Z., Mustafa, G., Komatsu, S., 2015. Plant responses to nanoparticle stress. Int. J. Mol. Sci. 16, 26644–26653.

Houston, K., Tucker, M.R., Chowdhury, J., Shirley, N., Little, A., 2016. The plant cell wall: a complex and dynamic structure as revealed by the responses of genes under stress conditions. Front. Plant Sci. 7, 984. https://doi.org/10.3389/fpls.2016.00984

Jiang, H.S., Yin, L.Y., Ren, N.N., Zhao, S.T., Li, Z., Zhi, Y., Shao, H., Li, W., Gontero, B., 2017. Silver nanoparticles induced reactive oxygen species via photosynthetic energy transport imbalance in an aquatic plant. Nanotoxicol. 11, 157–167.

Khajuria, A., Bali, S., Sharma, P., Kaur, R., Jasrotia, S., Saini, P., Ohri, P., Bhardwaj, R., 2019. S-Nitrosoglutathione (GSNO) and Plant Stress Responses. In: Mirza Hasanuzzaman, Vasileios Fotopoulos, Kamrun Nahar, Masayuki Fujita eds. Reactive Oxygen, Nitrogen and Sulfur Species in

Plants: Production, Metabolism, Signaling and Defense Mechanisms. John Wiley and sons Ltd. pp 627-644.

Kolbert, Zs., Pető, A., Lehotai, N., Feigl, G., Ördög, A., Erdei, L., 2012. *In vivo* and *in vitro* studies on fluorophore-specificity. Acta Biol. Szeged. 56, 37–41.

Kolbert, Zs., Feigl, G., Bordé, Á., Molnár, Á., Erdei, L., 2017. Protein tyrosine nitration in plants: Present knowledge, computational prediction and future perspectives. Plant Physiol. Biochem. 113, 56-63.

Kolbert, Zs., Molnár, Á., Szőllősi, R., Feigl, G., Erdei, L., Ördög, A., 2018. Nitro-oxidative stress correlates with se tolerance of *Astragalus* species. Plant Cell Physiol. 59, 1827–1843.

Kolbert, Zs., Oláh, D., Molnár, Á., Szőllősi, R., Erdei, L., Ördög, A., 2020. Distinct redox signalling and nickel tolerance in *Brassica juncea* and *Arabidopsis thaliana*. Ecotox. Environ. Saf. 189, 109989. https://doi.org/10.1016/j.ecoenv.2019.109989

Korkina, L.G., 2007. Phenylpropanoids as naturally occurring antioxidants: From plant defense to human health. Cell. Mol. Biol. 53, 15-25.

Kouhi, S.M.M., Lahouti, M., Ganjeali, A., Entezari, M.H., 2014. Comparative phytotoxicity of ZnO nanoparticles, ZnO microparticles, and Zn^{2+} on rapeseed (*Brassica napus* L.): investigating a wide range of concentrations. Toxicol. Environ. Chem. 96, 861-868.

Kouhi, S.M.M., Lahouti, M., Ganjeali, A., Entezari, M.H., 2015. Long-term exposure of rapeseed (*Brassica napus* L.) to ZnO nanoparticles: anatomical and ultrastructural responses. Environ. Sci. Pollut. Res. 22, 10733–10743.

Krzesłowska, M., 2011. The cell wall in plant cell response to trace metals: polysaccharide remodeling and its role in defense strategy. Acta Physiol. Plant. 33, 35–51.

Kumar, S.S., Venkateswarlu, P., Rao, V.R., Rao, G.N., 2013. Synthesis, characterization and optical properties of zinc oxide nanoparticles. Int. Nano Lett. 3, 30. https://doi.org/10.1186/2228-5326-3-30

Le Gall, H., Philippe, F., Domon, J.M., Gillet, F., Pelloux, J., Rayon, C.,2015. Cell wall metabolism in response to abiotic stress. Plants (Basel) 4, 112-166. https://doi/10.3390/plants4010112

Lehotai, N., Pető, A., Erdei, L., Kolbert, Zs., 2011. The effect of Se (Se) on development and nitric oxide levels in *Arabidopsis thaliana* seedlings. Acta Biol. Szeged. 55, 105–107.

Lehotai, N., Kolbert, Zs., Peto, A., Feigl, G., Ördög, A., Kumar, D., Tari, I., Erdei, L., 2012. Selenite-induced hormonal and signalling mechanisms during root growth of *Arabidopsis thaliana* L. J. Exp. Bot. 63, 5677–5687.

Lehotai, N., Lyubenova, L., Schröder, P., Feigl, G., Ördög, A., Szilágyi, K., Erdei, L., Kolbert, Zs., 2016. Nitro-oxidative stress contributes to selenite toxicity in pea *(Pisum sativum L)*. Plant Soil 400, 107-122.

Li, Y.-J., Chen, J., Xian, M., Zhou, L.-G., Han, F.X., Gan, L.-J., Shi, Z.-Q., 2014. In site bioimaging of hydrogen sulfide uncovers its pivotal role in regulating nitric oxide-induced lateral root formation. PLoS One 9, e90340. https://doi.org/10.1371/journal.pone.0090340

Li, Z.-G., Min, X., Zhou, Z.-H., 2016. Hydrogen Sulfide: a signal molecule in plant cross-adaptation. Front. Plant Sci. 7, 1621. https://doi.org/10.3389/fpls.2016.01621

Lin, D., Xing, B., 2007. Phytotoxicity of nanoparticles: inhibition of seed germination and root growth. Environ Pollut. 150, 243-250.

Loix, C., Huybrechts, M., Vangronsveld, J., Gielen, M., Keunen, E., Cuypers, A., 2017. Reciprocal interactions between cadmium-induced cell wall responses and oxidative stress in plants. Front. Plant Sci. 8, 1867. https://doi.org/10.3389/fpls.2017.01867

López-Moreno, M.L., de la Rosa, G., Hernández-Viezcas, J.A., Castillo-Michel, H., Botez, C.E., Peralta-Videa, J.R., Gardea-Torresdey, J.L., 2010. Evidence of the differential biotransformation and genotoxicity of ZnO and CeO2 nanoparticles on soybean *(Glycine max)* plants. Environ. Sci. Technol. 44, 7315-7320.

Lv, J., Zhang, S., Luo, L., Zhang, J., Yang, K., Christie, P., 2015. Accumulation, speciation and uptake pathway of ZnO nanoparticles in maize. Environ. Sci.: Nano. 2, 68. https://doi.org/10.1039/c4en00064a

Lv, J., Christie, P., Zhang, S., 2019. Uptake, translocation, and transformation of metal-based nanoparticles in plants: recent advances and methodological challenges. Environ. Sci.: Nano. 6, 41-59.

Ma, H., Williams, P.L., Diamond, S.A., 2013. Ecotoxicity of manufactured ZnO nanoparticles – A review. Environ. Pollut. 172, 76-85.

Marslin, G., Sheeba, C.J., Franklin, G., 2017. Nanoparticles alter secondary metabolism in plants *via* ROS burst. Front. Plant Sci. 8, 832. https://doi.org/10.3389/fpls.2017.00832

Michalak, A., 2006. Phenolic compounds and their antioxidant activity in plants growing under heavy metal stress. Pol. J. Environ. Stud. 15, 523-530.

Milner, M.J., Seamon, J., Craft, E., Kochian, L.V., 2013. Transport properties of members of the ZIP family in plants and their role in Zn and Mn homeostasis. J. Exp. Bot. 64, 369-381.

Mirzajani, F., Askari, H., Hamzelou, S., Schober, Y., Rompp, A., Ghassempour, A., Spengler, B., 2014. Proteomics study of silver nanoparticles toxicity on *Oryza sativa* L. Ecotoxicol. Environ. Saf. 108, 335–339.

Molnár, Á., Feigl, G., Trifán, V., Ördög, A., Szőllősi, R., Erdei, L., Kolbert, Zs., 2018a. The intensity of tyrosine nitration is associated with selenite and selenate toxicity in *Brassica juncea* L. Ecotox. Environ. Saf., 147: 93–101.

Molnár Á, Kolbert Zs, Kéri K, Feigl G, Ördög A, Szőllősi R, Erdei L (2018b) Selenite-induced nitro-oxidative stress processes in *Arabidopsis thaliana* and *Brassica juncea*. Ecotox. Environ. Saf. 148, 664-674.

Molnár, Á., Papp, M., Kovács, D.Z., Bélteky, P., Oláh, D., Feigl, G., Szőllősi, R., Rázga, Zs., Ördög, A., Erdei, L., Rónavári, A., Kónya, Z., Kolbert, Zs., 2020. Nitro-oxidative signalling induced by chemically synthetized zinc oxide nanoparticles (ZnO NPs) in *Brassica* species. Chemosphere 251, 126419. https://doi.org/10.1016/j.chemosphere.2020.126419

Mylona, Z., Panterise, E., Kevrekidis, T., Malea, P., 2020. Silver nanoparticle toxicity effect on the seagrass *Halophila stipulacea*. Ecotox. Environ. Saf. 189, 109925. https://doi.org/10.1016/j.ecoenv.2019.109925

Nair, P.M., Chung, I.M., 2014. Impact of copper oxide nanoparticles exposure on *Arabidopsis thaliana* growth, root system development, root lignificaion, and molecular level changes. Environ. Sci. Pollut. Res. Int. 21, 12709-12722.

Nair, R., Varghese, S.H., Nair, B.G., Maekawa, T., Yoshida, Y., Kumar, S.D., 2010. Nanoparticulate material delivery to plants. Plant Sci. 179, 154-163.

Parrotta, L., Guerriero, G., Sergeant, K., Cai, G., Hausman, J.-F., 2015. Target or barrier? The cell wall of early- and later-diverging plants vs cadmium toxicity: differences in the response mechanisms. Front. Plant Sci. 6, 133. https://doi.org/10.3389/fpls.2015.00133

Pérez-de-Luque, A., 2017. Interaction of nanomaterials with plants: What do we need for real applications in agriculture? Front. Environ. Sci. 5, 12. https://doi.org/10.3389/fenvs.2017.00012

Rahmani, F., Peymani, A., Daneshvand, E., Biparva, P., 2016. Impact of zinc oxide and copper oxide nano-particles on physiological and molecular processes in *Brassica napus* L. Ind. J. Plant Physiol. 21, 122–128.

Rahoui, S., Martinez, Y., Sakouhi, L., Ben, C., Rickauer, M., Rickauer, M., Ferjani, E.E., Gentzbittel, L., Chaoui, A., 2017. Cadmium-induced changes in antioxidative systems and differentiation in roots of contrasted *Medicago truncatula* lines. Protoplasma 254, 473–489.

Rogers, L.A., Dubos, C., Surman, C., Willment, J., Cullis, I.F., Mansfield, S.D., Campbell, M.M., 2005. Comparison of lignin deposition in three ectopic lignification mutants. New Phytol. 168, 123–140.

Sanz, L., Fernández-Marcos, M., Modrego, A., Lewis, D.R., Muday, G.K., Pollmann, S., Dueñas, M., Santos-Buelga, C., Lorenzo, O., 2014. Nitric oxide plays a role in stem cell niche homeostasis through its interaction with auxin. Plant Physiol. 166, 1972–1984.

Sarret, G., Harada, E., Choi, Y.E., Isaure, M.P., Geoffroy, N., Fakra, S., Marcus, M.A., Birschwilks, M., Clemens, S., Manceau, A., 2006. Trichomes of tobacco excrete zinc as zinc-substituted calcium carbonate and other zinc-containing compounds. Plant Physiol. 141, 1021–1034.

Schützendübel, A., Schwanz, P., Teichmann, T., Gross, K., Langenfeld-Heyser, R., Godbold, D.L., Polle, A., 2001. Cadmium-induced changes in antioxidative systems, hydrogen peroxide content, and differentiation in Scots pine roots. Plant Physiol. 127, 887-898.

Shaw, A.K., Hossain, Z., 2013. Impact of nano-CuO stress on rice (*Oryza sativa* L.) seedlings. Chemosphere 93, 906–915.

Shigeto, J., Tsutsumi, Y., 2016. Diverse functions and reactions of class III peroxidases. New Phytol. 209, 1395-1402.

Singh, A., Singh, N.B., Afzal, S., Singh, T., Hussain, I., 2018. Zinc oxide nanoparticles: a review of their biological synthesis, antimicrobial activity, uptake, translocation and biotransformation in plants. J. Mater. Sci. 53, 185–201.

Singh, A., Singh, N.B., Afzal, S., Singh, T., Hussain, I., 2018. Zinc oxide nanoparticles: a review of their biological synthesis, antimicrobial activity, uptake, translocation and biotransformation in plants. J. Material. Sci. 53, 185–201.

Singh, A., Singh, N.B., Hussain, I., Singh, H., 2017. Effect of biologically synthesized copper oxide nanoparticles on metabolism and antioxidant activity to the crop plants *Solanum lycopersicum* and *Brassica oleracea* var. botrytis. J. Biotechnol. 262, 11-27.

Soczynska-Kordala, M., Bakowska, A., Oszmianski, J., Gabrielska, J., 2001. Metal ion-flavonoid associations in bilayer phospholipid membranes. Cell. Mol. Biol. Lett. 6, 277-281.

Somssich, M., Khan, G.A., Persson, S., 2016. Cell wall heterogeneity in root development of *Arabidopsis*. Front. Plant Sci. 17, 1242. https://doi.org/10.3389/fpls.2016.01242

Srivastava, V., Gusain, D., Sharma, Y.C., 2013. Synthesis, characterization and application of zinc oxide nanoparticles (n-ZnO). Ceram. Int. 39, 9803-9808.

Sturikova, H., Krystofova, O., Huska, D., Adam, V., 2018. Zinc, zinc nanoparticles and plants. J. Hazard. Mat. 349, 101–110.

Takahama, U., Oniki, T., 2000. Flavonoids and some other phenolics as substrates of peroxidase: physiological significance of the redox reactions. J. Plant Res. 113, 301–309.

Talam, S., Karumuri, S.R., Gunnam, N., 2012. Synthesis, characterization, and spectroscopic properties of ZnO nanoparticles. ISRN Nanotechnol. 2012, 1-6. https://doi.org/10.5402/2012/372505

Tanou, G., Filippou, P., Belghazi, M., Job, D., Diamantidis, G., Fotopoulos, D., Molassiotis, A., 2012. Oxidative and nitrosative-based signaling and associated post-translational modifications orchestrate the acclimation of citrus plants to salinity stress. Plant J. 72, 585-599.

Tenhaken, R., 2014. Cell wall remodeling under abiotic stress. Front. Plant Sci. 5, 771. https://doi.org/10.3389/fpls.2014.00771

Thwala, M., Musee, N., Sikhwivhilu, L., Wepener, V., 2013. The oxidative toxicity of Ag and ZnO nanoparticles towards the aquatic plant *Spirodela punctata* and the role of testing media parameters. Environ. Sci. Process. 15, 1830–1843.

Tripathi, D.K., Singh, S., Singh, S., Srivastava, P.K., Singh, V.P., Singh, S., Prasad, S.M., Singh, P.K., Dubey, N.K., Pandey, A.C., Chauhan, D.K., 2017. Nitric oxide alleviates silver nanoparticles (AgNps)-induced phytotoxicity in *Pisum sativum* seedlings. Plant Physiol. Biochem. 110, 167–177.

Valderrama, R., Corpas, F.J., Carreras, A., Fernández-Ocaña, A., Chaki, M., Luque, F., Gómez-Rodríguez, M.V., Colmenero-Varea, P., del Río, L.A., Barroso, J.B., 2007. Nitrosative stress in plants. FEBS Lett. 581, 453–461.

Vandelle, E., Delledonne, M., 2011. Peroxynitrite formation and function in plants. Plant Sci. 181, 534-539.

Vannini, C., Domingo, G., Onelli, E., Prinsi, B., Marsoni, M., Espen, L., Bracale, M., 2013. Morphological and proteomic responses of *Eruca sativa* exposed to silver nanoparticles or silver nitrate. PLoS ONE 8, e68752. https://doi.org/10.1371/journal.pone.0068752

Vatén, A., Dettmer, J., Wu, S., Stierhof, Y.-D., Miyashima, S., Yadav, S.R., Roberts, C.J., Campilho, A., Bulone, V., Lichtenberger, R., Lehesranta, S., Mähönen, A.P., Kim, J.-Y., Jokitalo, E., Sauer, N., Scheres, B., Nakajima, K., Carlsbecker, A., Gallagher, K.L., Helariutta, Y., 2011. Callose biosynthesis regulates symplastic trafficking during root development. Dev. Cell 21, 1144-1155.

Voragen, A.G.J., Coenen, G.-J., Verhoef, R.P., Schols, H.A., 2009. Pectin, a versatile polysaccharide present in plant cell walls. Struct. Chem. 20, 263-275.

Wang, F., Liu, X., Shi, Z., Tong, R., Adams, C.A., Shi, X., 2016. Arbuscular mycorrhizae alleviate negative effects of zinc oxide nanoparticle and zinc accumulation in maize plants – A soil microcosm experiment. Chemosphere 147, 88-97.

Wang, P., Menzies, N.W., Lombi, E., McKenna, B.A., Johannessen, B., Glover, C.J., Kappen, P., Kopittke, P.M., 2013. Fate of ZnO nanoparticles in soils and cowpea *(Vigna unguiculata)*. Environ. Sci. Technol. 47, 13822−13830.

Xia, B., Chen, B., Sun, X., Qu, K., Ma, F., Du, M., 2015. Interaction of TiO_2 nanoparticles with the marine microalga *Nitzschia closterium*: growth inhibition, oxidative stress and internalization. Sci. Total Environ. 508, 525–533.

Xu, J., Yin, H., Li, Y., Liu, X., 2010. Nitric oxide is associated with long-term zinc tolerance in *Solanum nigrum*. Plant Physiol. 154, 1319-1334.

Yanık, F., Vardar, F., 2015. Toxic effects of aluminum oxide (Al_2O_3) nanoparticles on root growth and development in *Triticum aestivum*. Water Air Soil Pollut. 226, 296. https://doi.org/10.1007/s11270-015-2566-4

Zafar, H., Ali, A., Ali, J.S., Haq, I.U., Zia, M., 2016. Effect of ZnO nanoparticles on *Brassica nigra* seedlings and stem explants: growth dynamics and antioxidative response. Front. Plant Sci. 20, 535. https://doig.org/10.3389/fpls.2016.00535

Zelko, I., Lux, A., Sterckeman, T., Martinka, M., Kollárová, K., Lišková, D., 2012. An easy method for cutting and fluorescent staining of thin roots. Ann. Bot. 110, 475–478.

Zhang, X., Qin, J., Xue, Y., Yu, P., Zhang, B., Wang, L., Liu, R., 2014. Effect of aspect ratio and surface defects on the photocatalytic activity of ZnO nanorods. Sci. Rep. 4, 4596. https://doi.org/10.1038/srep04596

Figure captions

Fig 1 ZnO NPs affect root biomass production of *Brassica* seedlings. Primary root length (cm, A), root fresh weight (mg, B) and root width (µm, C) of control (0 mg/L ZnO NP), 25 or 100 mg/L ZnO NP-exposed 5-day-old *Brassica napus* and *Brassica juncea* seedlings. Different letters indicate significant differences according to Duncan's test (n=20, $p<0.05$). (D) Representative photographs taken from *Brassica* seedlings (three seedlings/treatment) grown in the absence (0 mg/L ZnO NP) or in the presence of 25 or 100 mg/L ZnO NP. Bars=2 cm. (E) Cross sections prepared from the differentiation zone of primary roots of control and ZnO NP-treated Brassica seedlings. Bars= 250 µm.

Fig 2 ZnO NPs affect root cell viability of *Brassica* seedlings. Viability of root meristem cells (pixel intensity of fluorescein fluorescence, control%) in roots of 5-day-old *Brassica napus* and *Brassica juncea* seedlings grown in Petri dishes supplemented with 0, 25 or 100 mg/L ZnO NP. Different letters indicate significant differences according to Duncan's test (n=10, $p<0.05$). (B) Representative fluorescent microscopic images of FDA-stained root tips of control and ZnO NP-treated *Brassica* seedlings. Bars=250 µm.

Fig 3 ZnO NPs induce Zn^{2+} accumulation and ZnO NPs may be bounded in the cell walls. The level of free, intracellular Zn^{2+} (pixel intensity of Zinquin fluorescence, A) in the root tips of 5-day-old *Brassica napus* and *Brassica juncea* seedlings grown in the absence (0 mg/L ZnO NP) or in the presence of ZnO NP (25 or 100 mg/L). Different letters indicate significant differences according to Duncan's test (n=10, $p<0.05$). (B) Representative microscopic photographs taken from the root tips of control or ZnO NP-treated *Brassica* seedlings. Bars=250 µm. (C) TEM images of root (C, bars=1 µm) and hypocotyl (D, bars=500 nm, upper row and 1 µm lower row) cells of *Brassica* species treated with 0, 25 or 100 mg/L ZnO NPs. White arrows indicate electron dense cell wall in a root cell of 25 mg/L ZnO NP-treated *B. napus*.

Fig 4 ZnO NPs induces alterations in cell wall composition. Callose level (pixel intensity of aniline blue-associated fluorescence, A) and microscopic images taken from aniline blue-stained root tips (B) of 5-days-old *Brassica napus* and *Brassica juncea* treated with 0, 25 or 100 mg/L ZnO NP. Different letters indicate significant differences according to Duncan's test (n=10, $p<0.05$). Bars= 250 µm. (C) Representative microscopic images of control and ZnO NP-treated *Brassica* roots stained with phloroglucinol. Reddish brown discoloration indicates lignification. Bars= 250 µm. (D) Representative microscopic images of control and ZnO NP-treated *Brassica* roots stained with Ruthenium Red. Pink discoloration indicates pectin. Bars= 250 µm. (E) Values of lignin and suberin levels (pixel intensity) in the roots of *Brassica* seedlings treated with 0, 25 or 100 mg/L ZnO NP. Different letters indicate significant differences according to Duncan's test (n=10, $p<0.05$). (F) Representative images of Auramine-O-stained root cross sections. Bars=250 µm.

Fig 5 Cell wall-related defence in *Brassica* roots is induced by ZnO NPs. Quercetin levels (pixel intensity of flavonol-specific DPBA fluorescence) in the root tips of *Brassica napus* and *Brassica juncea* grown in the absence (0 mg/L ZnO NP) or in the presence of 25 or 100 mg/L ZnO NP for 5 days. Different letters indicate significant differences according to Duncan's test (n=10, $p<0.05$). (B) Representative images taken from DPBA-labelled roots of *Brassica* seedlings. Bars=250 µm. (C) Pyrogallol staining of *Brassica* root tips indicating the activity of cell wall peroxidases. Bars=250 µm.

Fig 6 ZnO NPs disturb ROS and RNS homeostasis in *Brassica* roots. The levels of H_2O_2 (pixel intensity of ADHP-associated fluorescence, A), $O_2^{\cdot -}$ (pixel intensity of DHE-associated fluorescence, B), H_2S (pixel intensity of WSP1-associated fluorescence, C), NO (pixel intensity of DAF FM-associated fluorescence, D), $ONOO^-$ (pixel intensity of DAF FM-associated fluorescence, E) and GSNO (pixel intensity of FITC-associated fluorescence, F) in roots of control and 25 or 100 mg/L ZnO NP-treated *Brassica napus* and *Brassica juncea*. Different letters indicate significant differences according to Duncan's test (n=10, $p<0.05$). (G) Representative fluorescent microscopic images

showing root tips of control and ZnO NP-treated Brassica seedlings labelled with ADHP, DHE, DAF-FM and anti-GSNO. Bars= 250 µm.

Fig 7 ZnO NPs induce protein nitration and lipid peroxidation in roots of *Brassica*. Levels of 3-nitro-tyrosine (NO_2-Tyr)-associated fluorescence (pixel intensity, A) in root cross sections of 5-days-old *Brassica napus* and *Brassica juncea* seedlings treated with 0, 25 or 100 mg/L ZnO NP. Different letters indicate significant differences according to Duncan's test (n=10, $p<0.05$). (B) Representative images showing root cross sections immunolabelled for NO_2-Tyr. Bars=250 µm. (C) Schiff-reagent-labelled root tips of Brassica seedlings treated with 0, 25 or 100 mg/L ZnO NP. Pink discoloration indicates lipid peroxidation. Bars=250 µm.

Figure 1

Click here to access/download;Figure;Fig 1_300.tif

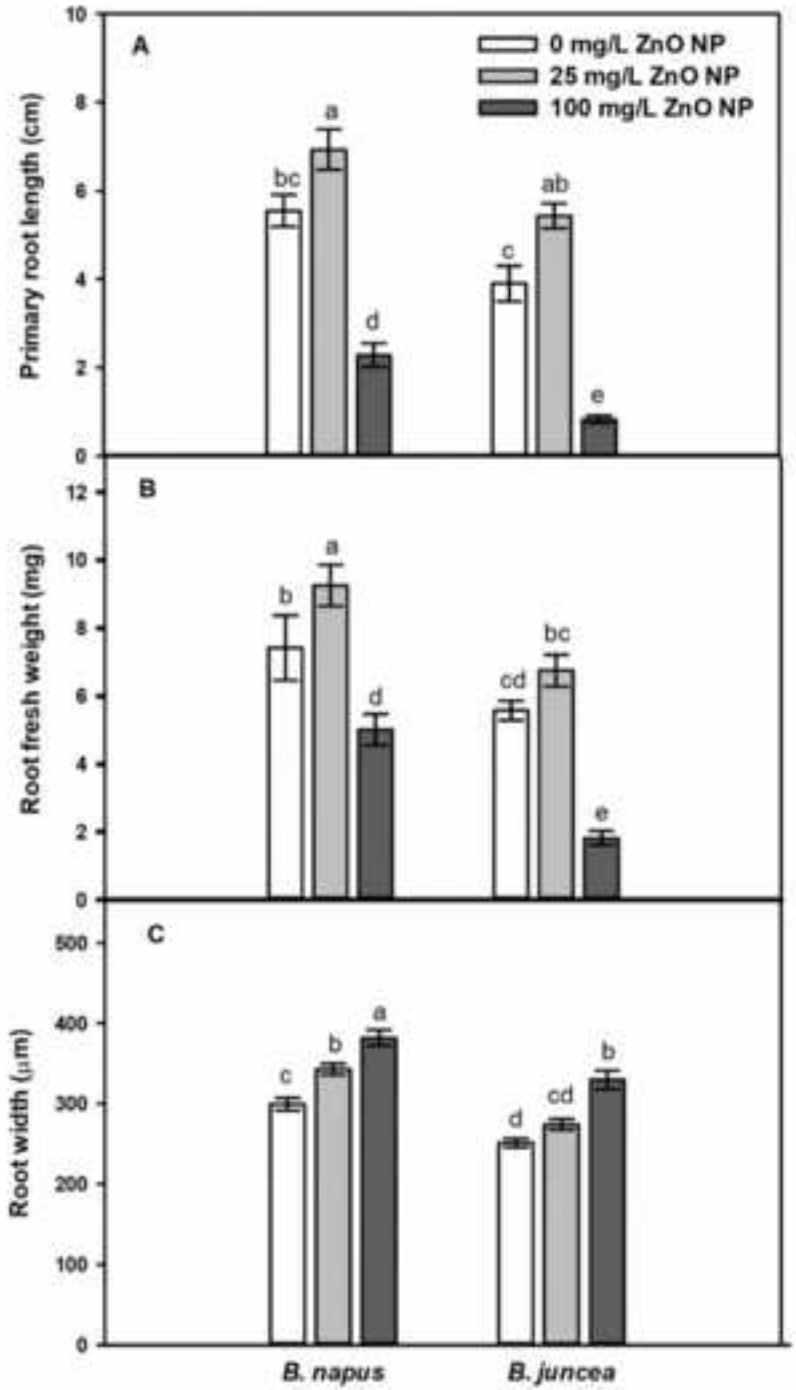

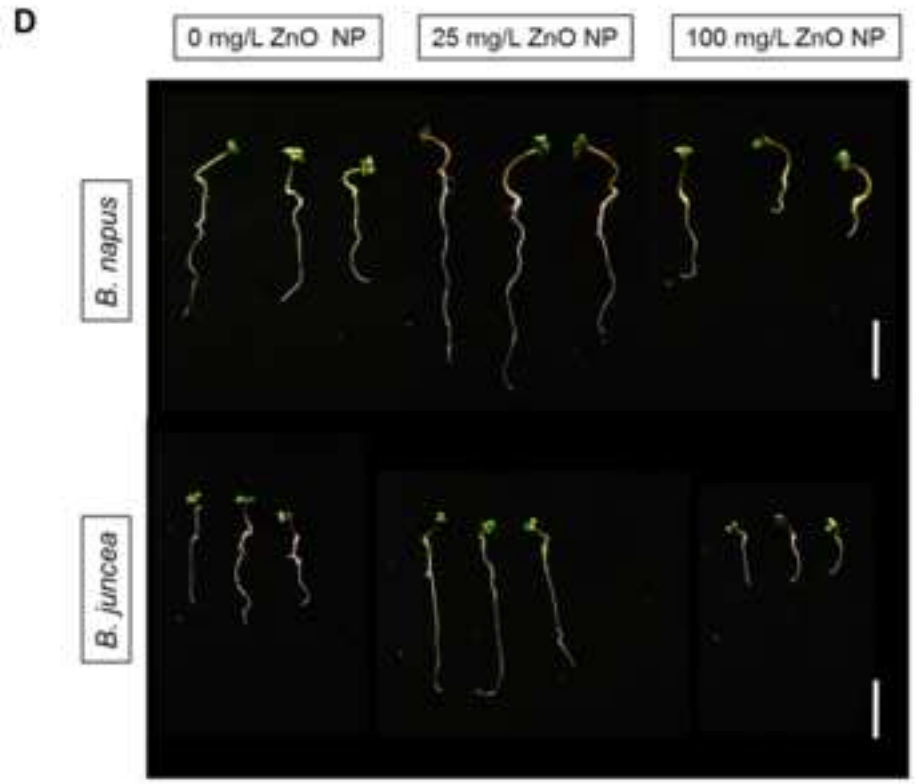

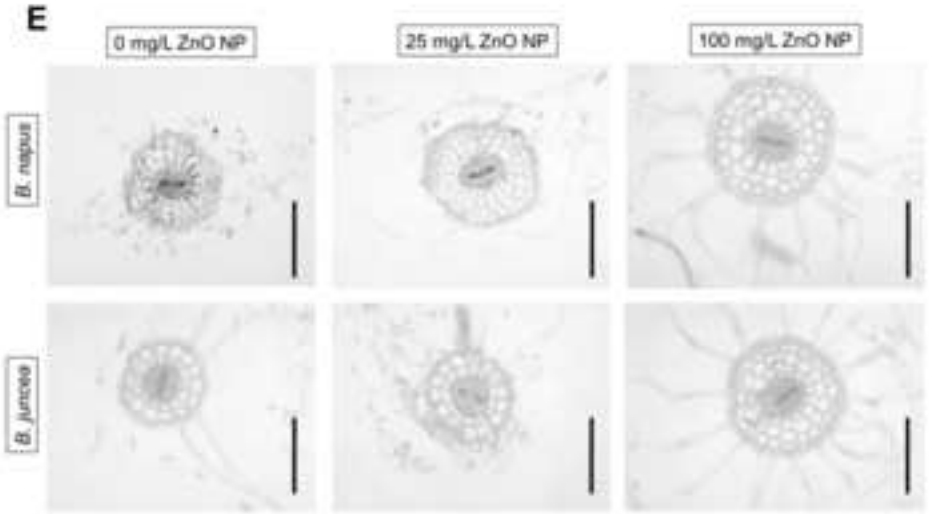

Figure 2

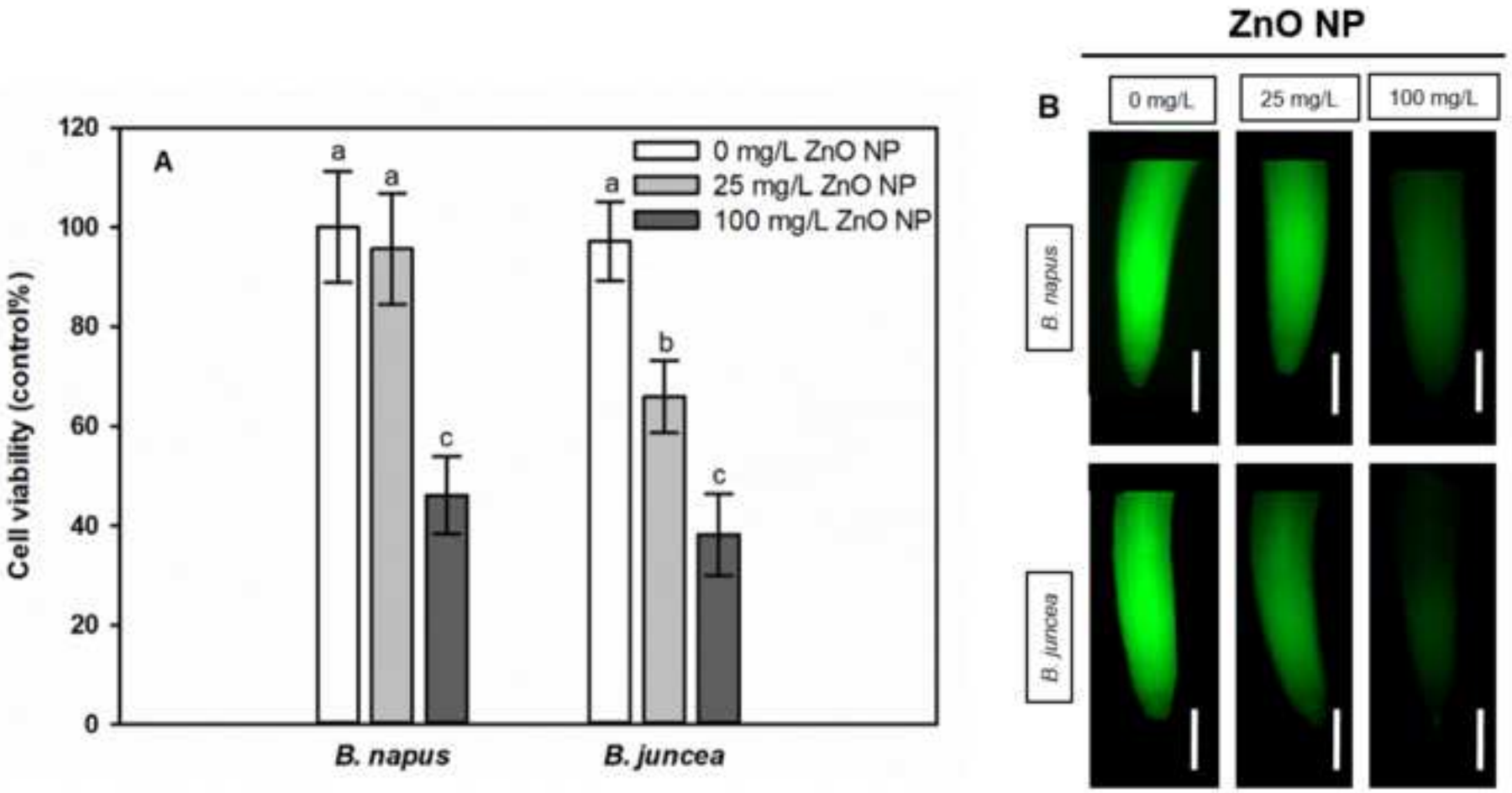

Figure 3

Click here to access/download;Figure;Fig 3_300.tif

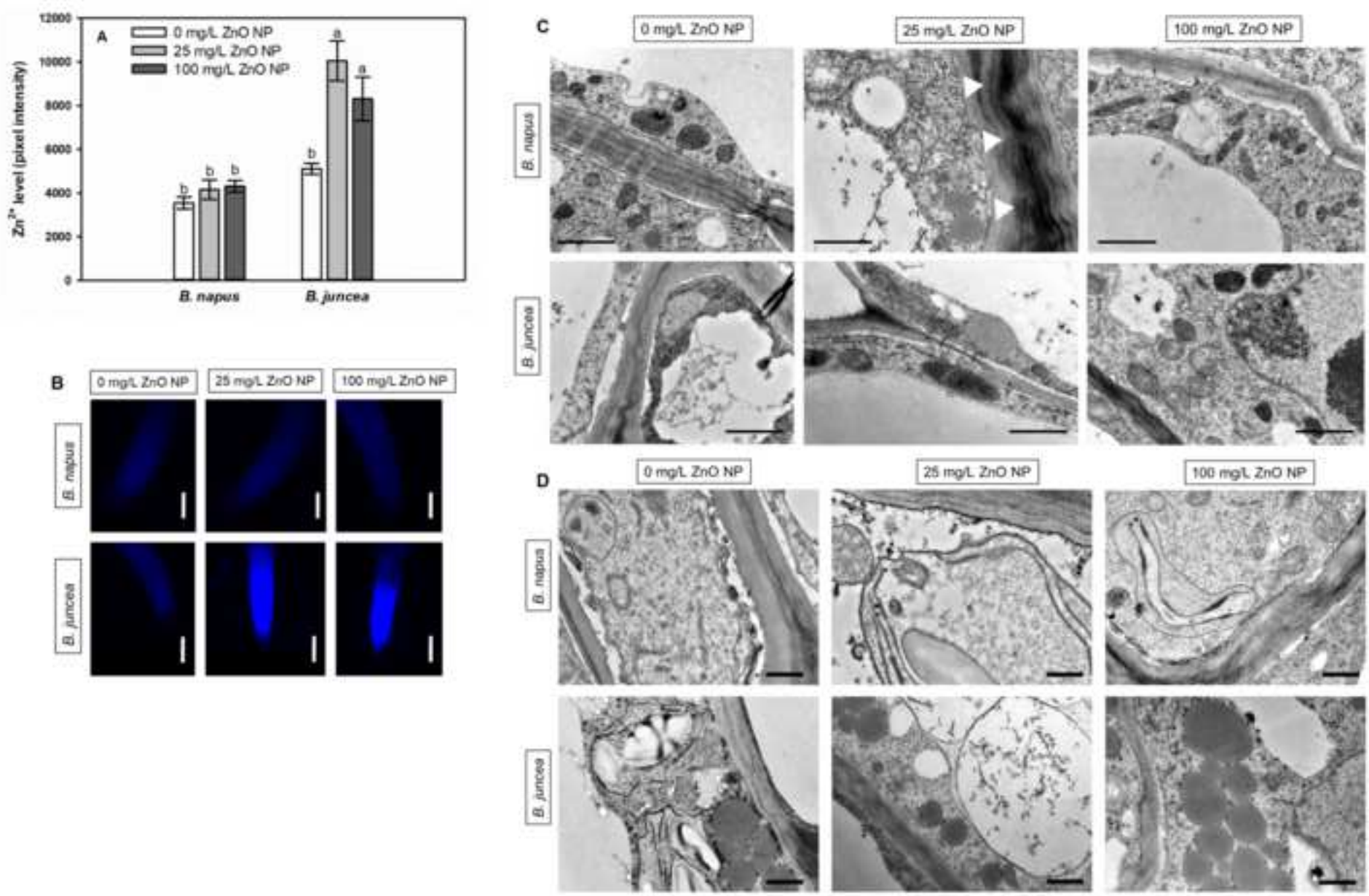

Figure 4

Click here to access/download;Figure;Fig 4_300.tif

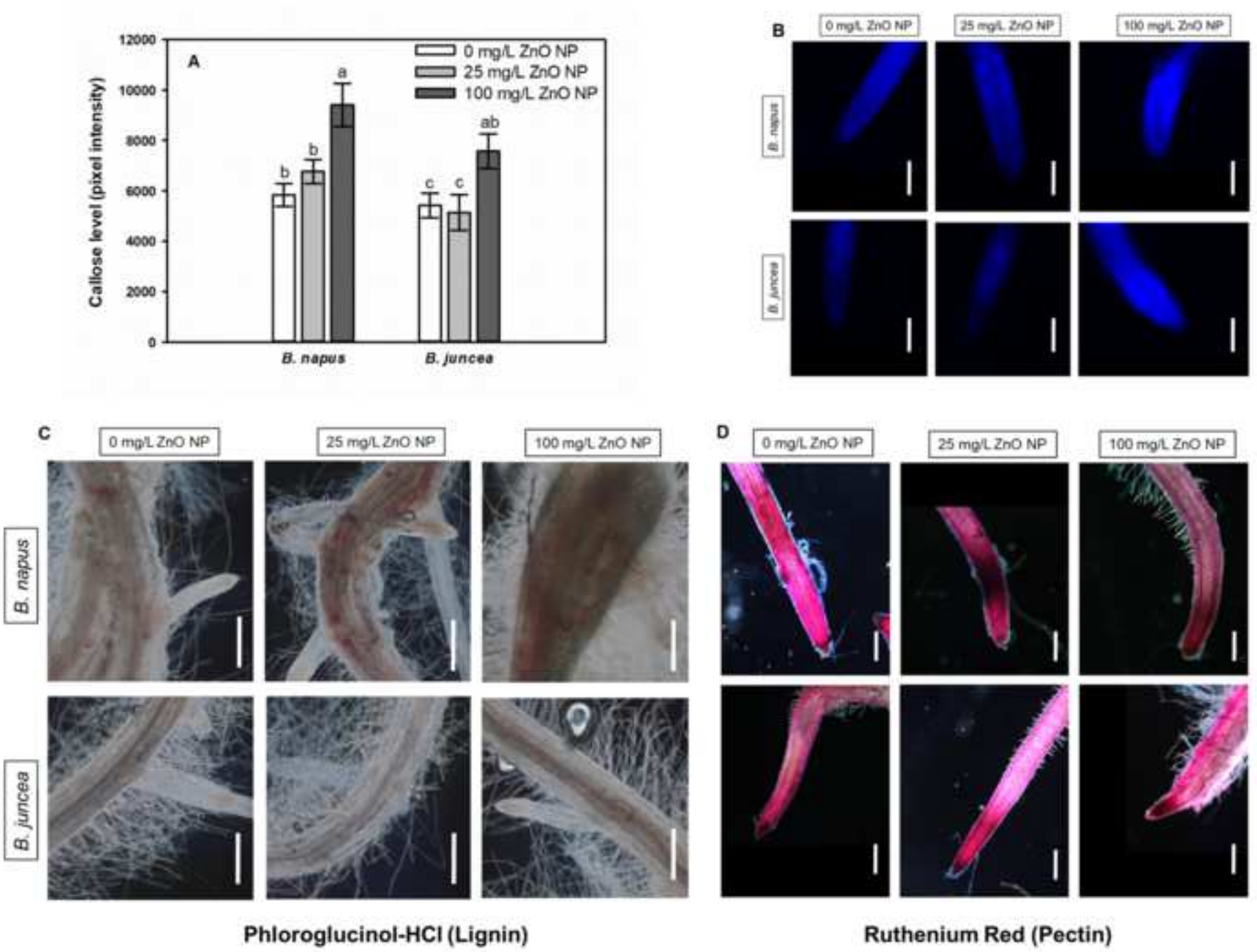

Figure 5

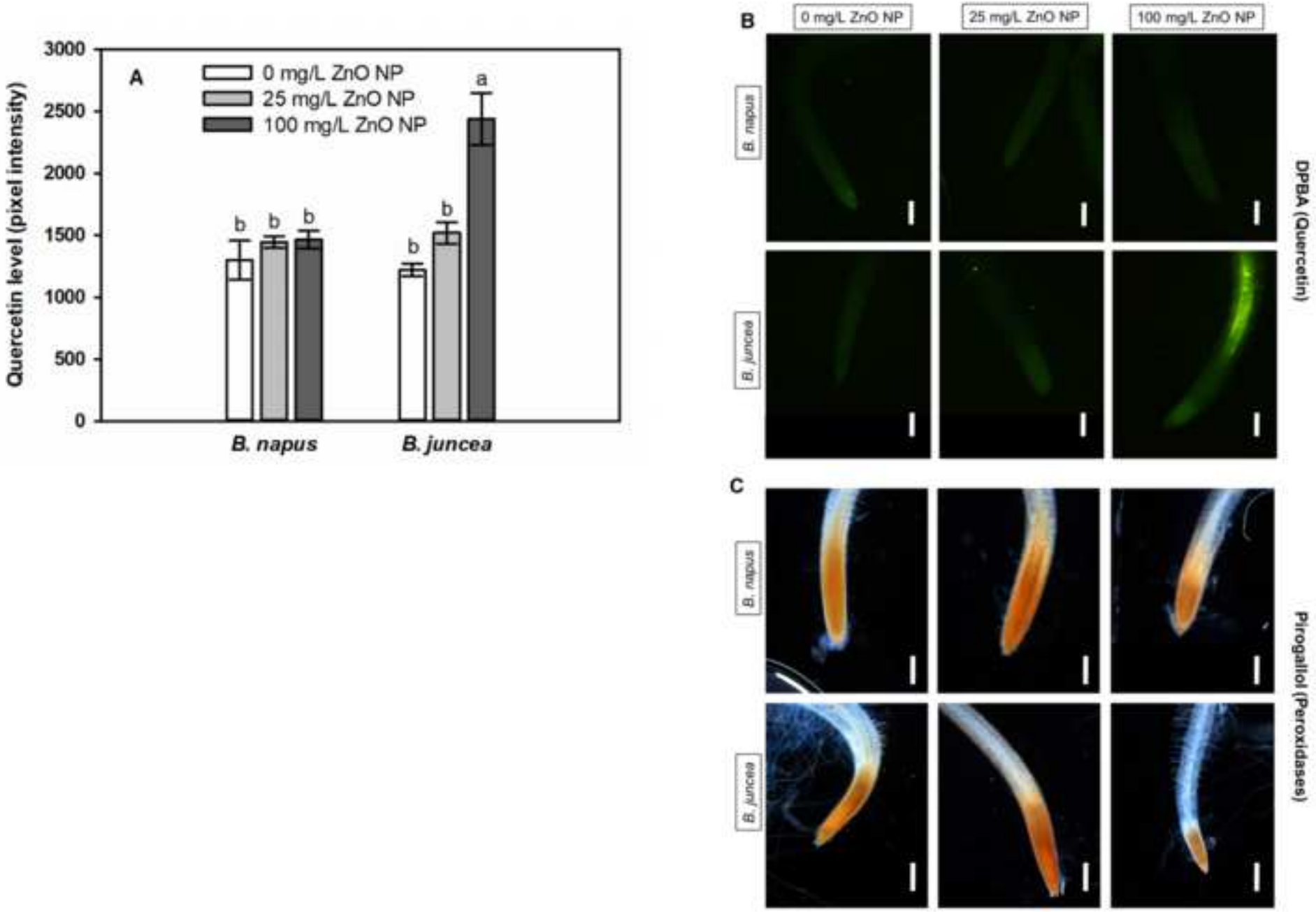

Figure 6

Click here to access/download;Figure;Fig 6_300.tif

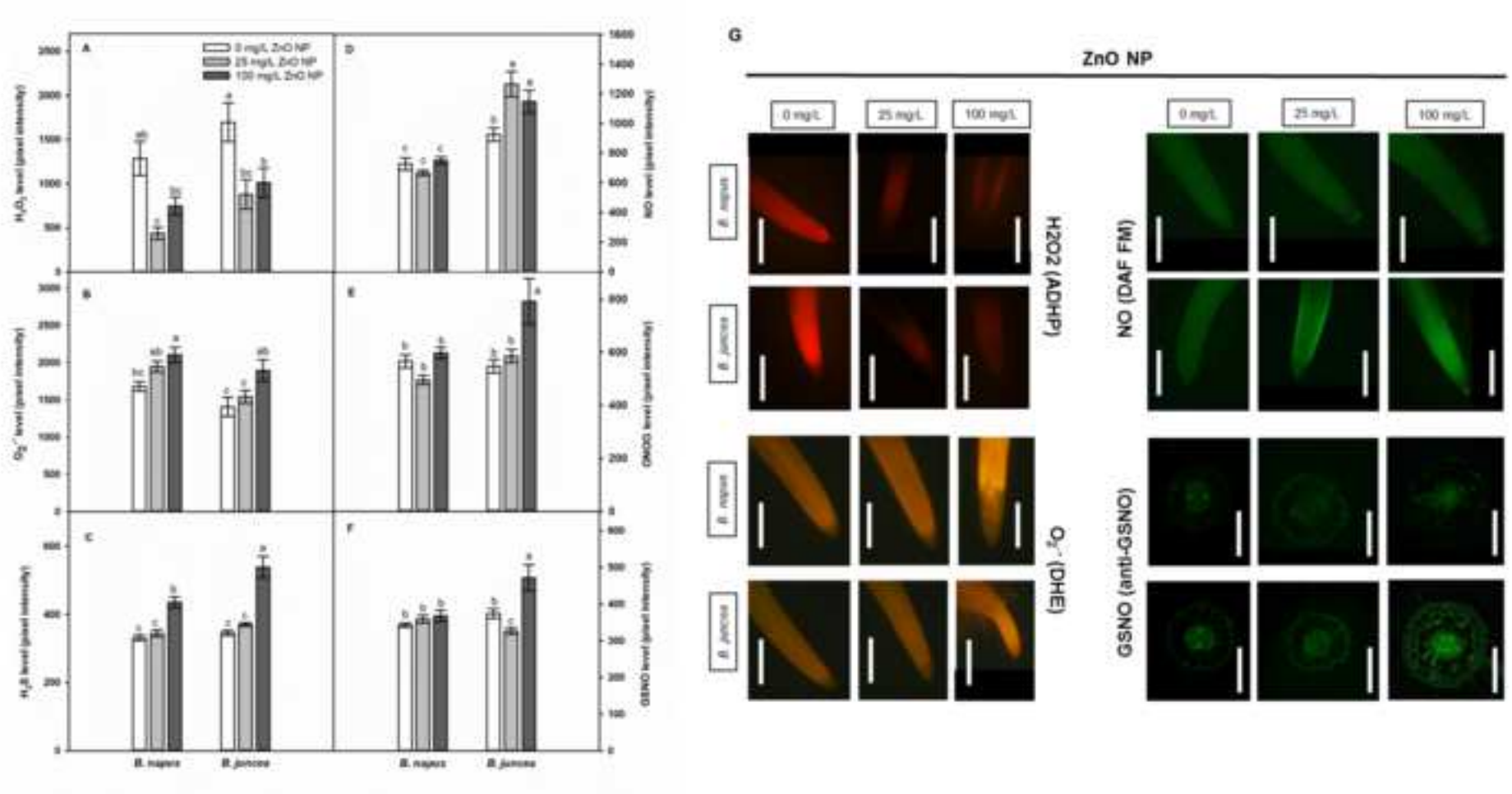

Figure 7

Click here to access/download;Figure;Fig 7_300.tif

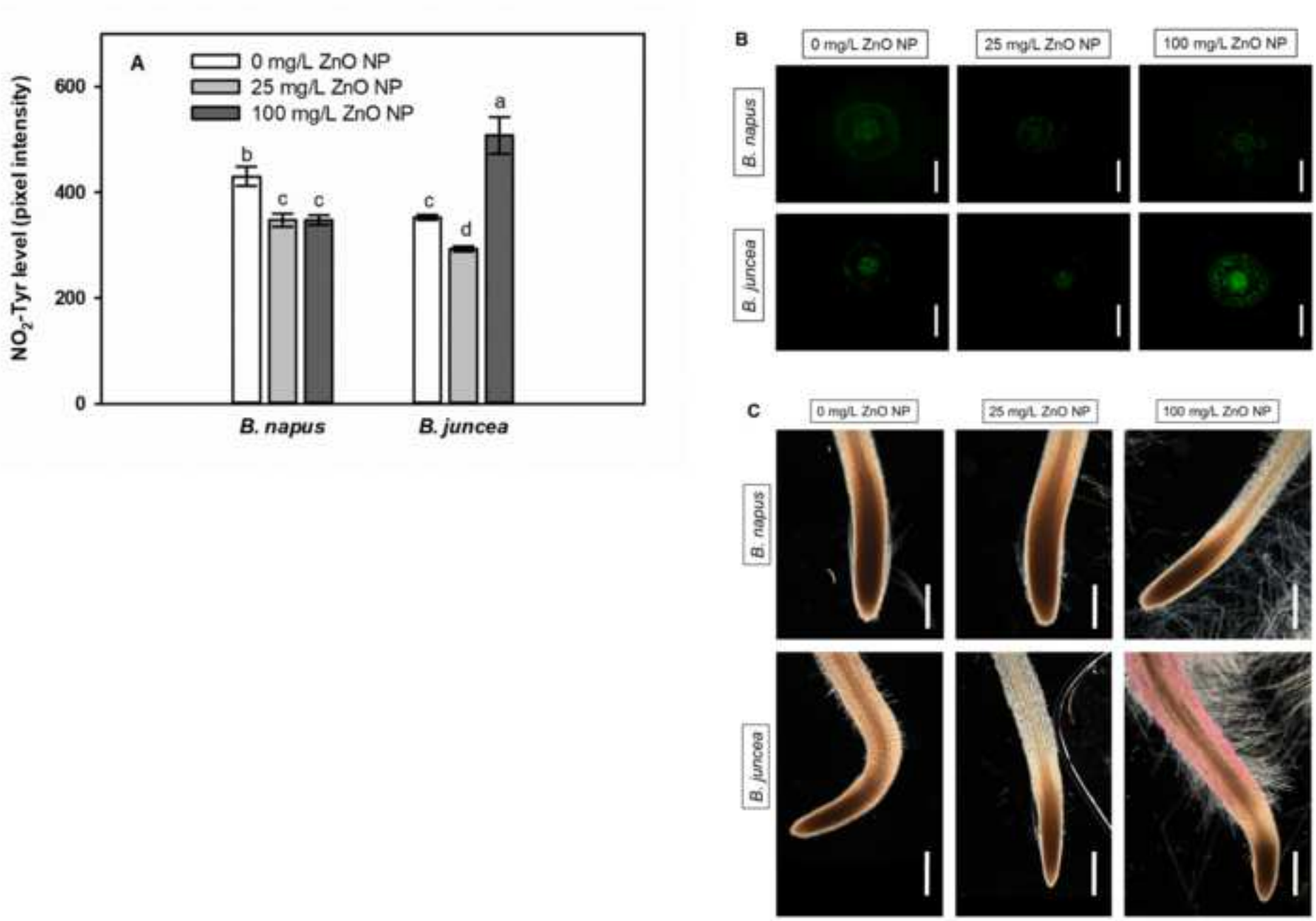

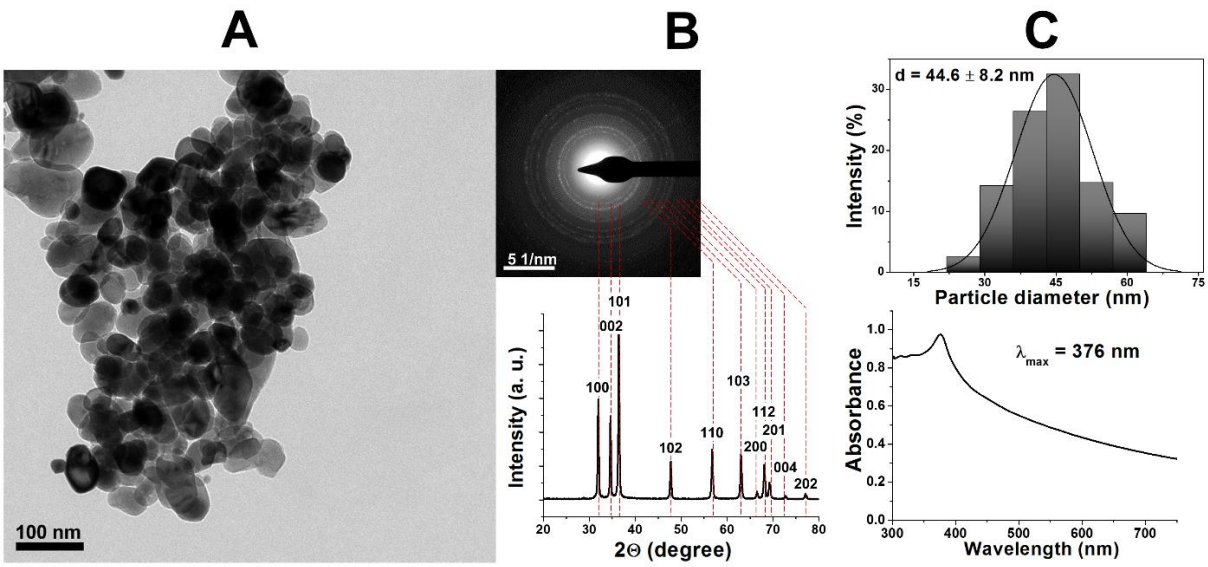

Fig 1 Chemical characterization of zinc oxide nanoparticles. Transmission electron microscopic (TEM) image (A), with the corresponding (B) electron diffraction (ED) pattern (top) and X-ray diffractogram (XRD) (bottom) of the synthesized particles with highlighted characteristic Miller indices, furthermore their (C) particle size distribution histogram (top) and UV-Vis spectrum (bottom).

Credit author statement

Árpád MOLNÁR, Investigation; Methodology; Roles/Writing - original draft

Andrea RÓNAVÁRI, Investigation; Methodology; Writing - review & editing

Péter BÉLTEKY, Investigation; Methodology

Réka SZŐLLŐSI, Investigation; Methodology; Writing - review & editing

Emil VALYON, Investigation

Dóra OLÁH, Investigation

Zsolt Rázga, Investigation; Methodology; Writing - review & editing

Attila ÖRDÖG, Writing - review & editing

Zoltán KÓNYA, Funding acquisition; Writing - review & editing

Zsuzsanna KOLBERT, Conceptualization; Funding acquisition; Visualization; Supervision; Writing - review & editing

Declaration of interests

☒ The authors declare that they have no known competing financial interests or personal relationships that could have appeared to influence the work reported in this paper.

☐The authors declare the following financial interests/personal relationships which may be considered as potential competing interests: